Available online at www.sciencedirect.com
SCIENCE DIRECT®
Coordination Chemistry Reviews 248 (2004) 1061–1083
COORDINATION CHEMISTRY REVIEWS
www.elsevier.com/locate/ccr

Review

Structural chemistry and properties of metal arenesulfonates

Jiwen Cai*

School of Chemistry and Chemical Engineering, Sun Yat-Sen University, Guangzhou 510275, PR China

Received 20 February 2004; accepted 24 June 2004

Contents

Abstract

Recent progress in the solid-state coordination and structural chemistry of aromatic disulfonates as well as the amine interaction properties of crystalline Cd^{2+} sulfonate complexes will be outlined. Due to the weak coordination strength, most of the metal monosulfonates obtained from aqueous solution are water-coordinated metal sulfonate salts. However, by employing arenedisulfonates, which can provide multiple coordination sites, stable frameworks sustained by sulfonate–metal interactions can be obtained with various dimensionalities. The sulfonate groups show diverse coordination modes, which change starkly from η^3 μ^3 bridging in sodium(I) 1,5-naphthalenedisulfonate dihydrate to η^7 μ^5 bridging in sodium(I) 4,4′-phenyletherdisulfonate. The coordination strength of the alkali, alkaline earth metals and some divalent transition metals toward sulfonates will be evaluated. Moreover, layered sulfonate- and water-coordinated Cd^{2+} complexes can selectively uptake amine vapor via solid-state substitution reaction, in a reversible process under ambient conditions. The coordination modes and conformations of aromatic monosulfonates are analyzed based upon the crystal structures documented by CSD. The *syn* monodentate mode is most frequently adopted.

Keywords: Sulfonate; Coordination chemistry; Alkali metal; Alkaline earth metal; Transition metal; Solid–vapor reaction

* Tel.: +86 20 84114215; fax: +86 20 84112245.
E-mail address: puscjw@zsu.edu.cn (J. Cai).

0010-8545/$ – see front matter © 2004 Elsevier B.V. All rights reserved.
doi:10.1016/j.ccr.2004.06.014

1. Introduction

1.1. Background

In comparison with other organic acidato anions such as carbonates and phosphonates, the coordination chemistry of sulfonate has been less well investigated due to the perception that sulfonate is a poor ligand [1]. The supramolecular chemistry of the sulfonate group in extended solids constructed by cooperative coordination and other weak intermolecular interactions, as well as the structural and functional properties of Ba^{2+} and Ag^{+} sulfonates, have recently been reviewed by Côté and Shimizu [1]. The coordination chemistry of the trifluoromethanesulfonate was reviewed by Lawrence [2], while polysulfonate calyx [4]- and calyx [5] arenas were reviewed by Atwood et al. [3]. This manuscript will focus on the variant and preferential coordination modes displayed by aromatic mono- and disulfonates. The recent progress made in our group in the structural chemistry of metal arenedisulfonates as well as the amine interaction properties of cadmium(II) sulfonates will be summarized.

1.2. Coordination modes of aromatic sulfonates

In contrast to phosphonates which form mostly rigid inorganic–organic lamellar frameworks with the organic pendant protruding from the inorganic $–PO_3$-M layers [4], the structural analogs, sulfonates, show diverse coordination behavior. The weak coordination nature of $–SO_3^{-}$ makes its coordination mode very flexible and sensitive to the chemical environment. For instance, the coordination modes of $–SO_3^{-}$ to Na^{+} range from $\eta^3\ \mu^3$ bridging in sodium(I) 1,5-naphthalenedisulfonate dihydrate [5] to $\eta^7\ \mu^5$ in sodium(I) 4,4′-biphenyletherdisulfonate [6]. Similar observations have also been made in the silver(I) sulfonates [7,8].

The CSD, released in October 2003, has documented a few dozen crystal structures of aromatic sulfonate-coordinated metal complexes, with different kinds of metals scattered around the Periodic Table [7–68]. The most frequently found ligands for forming sulfonate–metal interactions are listed in Fig. 1. All these complexes are either mixed-ligand coordinated by the hard sulfonate group together with some other softer ligands such as nitrogen-, sulfur- or phosphorus-containing molecules (X), or the metal ions are hydrated. In most of these compounds, the sulfonate groups adopt the monodentate coordination mode. For instance, in a variant of organometallic compounds, including Sb^{5+} [9–18], Bi^{5+} [11,19], Sn^{4+} [20,21], Tc^{+} [22], Ru^{2+} [23], Rh^{+} [24,25], Pd^{2+} [26], Ag^{+} [27], and Re^{2+} [28] ions, besides the carbon-coordinated organic ligands, the metal ions are also coordinated by a monodentate $C_6H_5SO_3^{-}$ ligand or its substituted analogs (L1). In the coordination compounds, including Cu^{2+} [29–31], Zn^{2+} [32], Ni^{2+} [33], Ag^{+} [34–37], Au^{+} [38], Fe^{2+} [39,40], Ru^{2+} [41], Pd^{2+} [42], and W^{2+} [43] ions, the metal ions are coordinated by L1 together with the nitrogen-, sulfur- or phosphorus-containing ligands (X), or by the multi-functional ligands L2 and L3. $NH_2C_6H_4SO_3^{-}$ (L1) adopts the O- or N,O-coordination modes with Mn^{2+} [44], Co^{2+} [45], Zn^{2+} [45], Mo^{2+} [46], and Tl^{+} [47]. The hard nature of the sulfonate group seems to favor the hard rare-earth metal ions and a series of lanthanide sulfonates are isolated from aqueous solution with the Ln ions coordinated by both the water molecules and sulfonates [48–56].

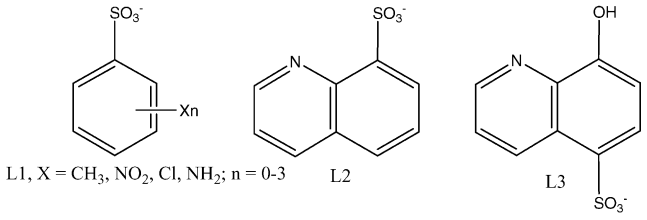

Fig. 1. The aromatic sulfonate ligands.

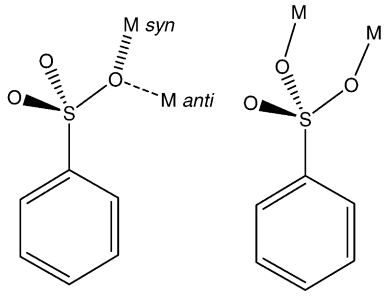

Fig. 2. The mono and $\eta^2\ \mu^2$ bidentate coordination modes of aromatic sulfonate.

Among the bidentate modes adopted by sulfonate, the O,O′-$\eta^2\ \mu^2$ bridging, as shown in Fig. 2, is the most popular one which could also construct polymeric coordination networks with different topologies [34,47,57–65]. For example, an 8-membered ring is built [57,58,61], as shown in Fig. 3, by two $\eta^2\ \mu^2$ sulfonates coordinated to two metal ions. The 8-membered-ring building blocks can further be extended into a 1D chain if the metal ions are connected to four sulfonate groups [59,60], as shown in Fig. 4. 1D coordination polymers can be generated with different topologies [34,59,61–63], as shown in Fig. 5. Other higher-order coordination modes are mostly observed in the silver(I) [7,8,34,47,64,65] sulfonates and have been reviewed by Côté and Shimizu [1].

Finally, there are only a few structural reports on disulfonate coordination compounds, with both sulfonate groups coordinated to metal ions. In the mixed-ligand complexes $[K(OH_2)_2M\{o\text{-}C_6H_4(SO_3)_2\}_2]_n$ (M = Nd and La) and $[K(OH_2)_2Yb(OH_2)_4\{o\text{-}C_6H_4(SO_3)_2\}_2]_n$ [66], there are two or more individual $o\text{-}C_6H_4(SO_3)_2$ ligands present in which most of the sulfonate oxygen atoms coordinate to K^{+}, Ln^{3+} or both of them in different bridging modes, as shown in Fig. 6. While in the series of lanthanide 1,5-naphthalenedisulfonate complexes $[Ln(OH)(1,5nds)(H_2O)]_n$ (Ln = La, Pr and Nd) [67], the disulfonate ligands are coordinated by five different Ln ions in a unusual asymmetrical $\eta^2\ \mu^2\ –\eta^3\ \mu^3$ mode, as

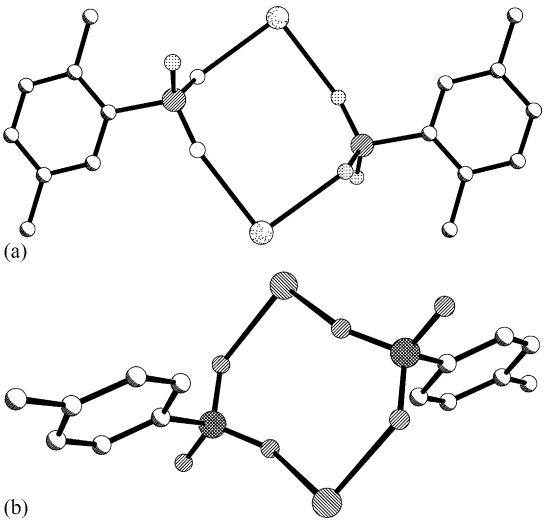

Fig. 3. The 8-membered-ring dimmers formed by two η^2 μ^2 sulfonate groups, coordinated via *syn–syn* modes in $Bi[((CH_3)_2C_6H_3SO_3)(C_6H_5)Cl_2]Sb(C_6H_5)_4$ [57] (a), via *syn–anti* modes in $Ag_2[(CH_3C_6H_4SO_3)_2((CH_3)_2NHC_4N_2H)_3]$ [34] (b).

shown in Fig. 7, resulting in stable polymeric structure with bifunctional catalysis and optical properties.

Besides the bridging modes, the *syn* or *anti* coordination conformation, defined by the M-O direction relative to the C-S bond, is another variable used to describe the coordination modes of the sulfonates, as defined and discussed by Sundberg and Sillanpää [68] for the mono-coordinated aromatic sulfonates. Among the 63 mono-coordinated metal sulfonate structures we examined [9–56], only nine of them adopt the *anti* coordination mode. Some of the *anti* conformations are accompanied by a second functional group coordinated to the metal ion which could be responsible for forcing the sulfonate oxygen to coordinate in the *anti* mode. Therefore, the *syn* coordination mode is preferred for mono-coordinated aromatic sulfonates. In the case of the η^2 μ^2 bidentate bridging, there are equal number of *anti* and *syn* modes observed. For instance, in the centro-symmetric 8-membered ring constituted by two sulfonate groups in η^2 μ^2 modes, the two independent sulfonate oxygen atoms could coordinate in a *syn–syn* fashion as shown in Fig. 3a, or *syn–anti* fashion as shown in Fig. 3b. While in the 1D chains constructed by the sulfonate groups coordinated in η^2 μ^2 bridging, the coordination modes could be *syn–syn* as shown in Fig. 5a, *syn–anti* as shown in Fig. 5b, *anti–anti* as shown in Fig. 5c. Strong π–π interactions are observed in $\{Pb[(CH_3C_6H_4SO_3)_2(C_6H_5)_2(H_2O)_2](H_2O)\}_n$ [62], as indicated by the coplanarity of the phenyl rings in Fig. 5c. This observation indicates that intermolecular interaction could play an important role in determining the *syn*

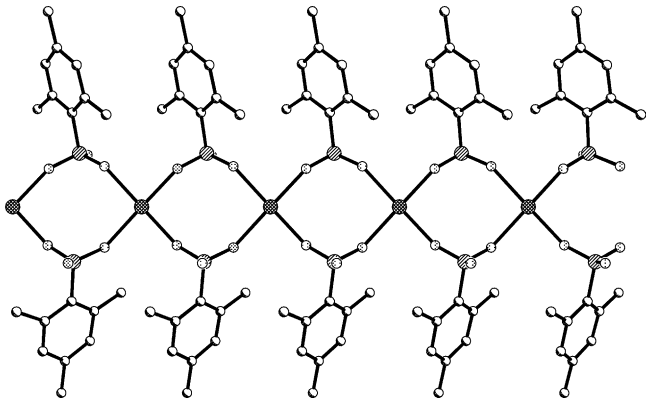

Fig. 4. The 1D chain constructed by 8-membered rings in $[(n\text{-}C_4H_9)_2Sn\{\mu\text{-}OSO_2C_6H_2(CH_3)_3\}_2]_n$ [59].

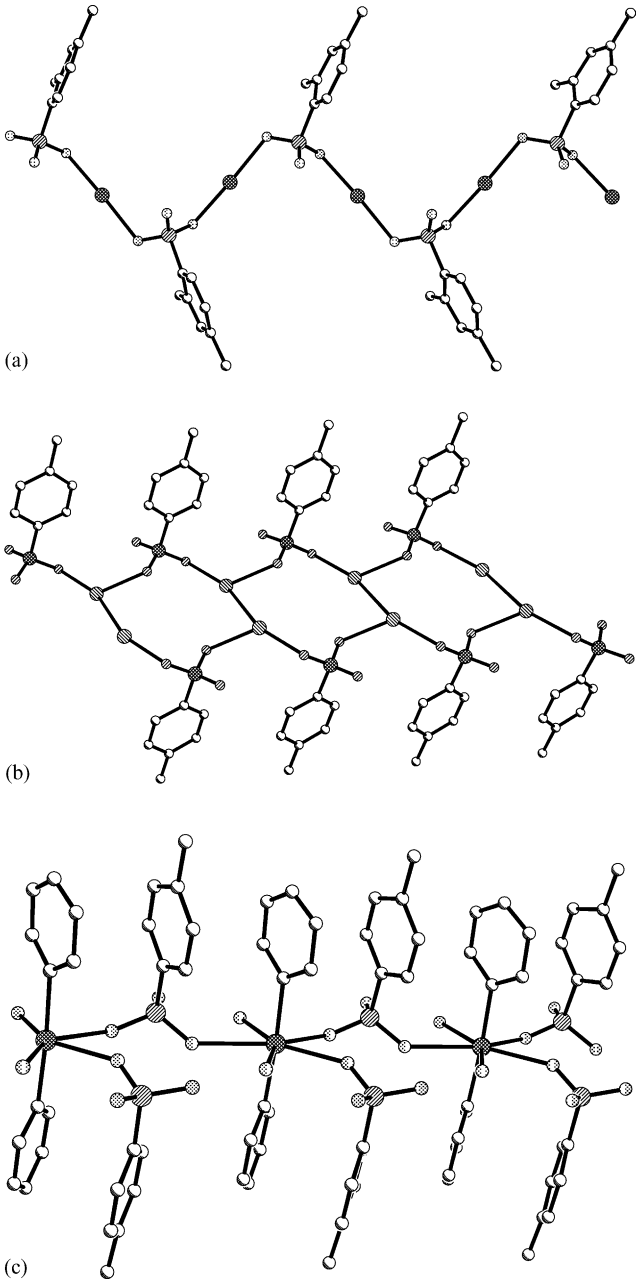

Fig. 5. The 1D chain constructed by the η^2 μ^2 sulfonate groups coordinated via *syn–syn* modes, in $Bi[((CH_3)_2C_6H_3SO_3)(C_6H_5)_2]$ [61] (a), via *syn–anti* modes in $Ag[(CH_3C_6H_4SO_3)((H_2N)_2C_5NH_3)]$ [63] (b), and via *anti–anti* in $Pb[(CH_3C_6H_4SO_3)_2(C_6H_5)_2(H_2O)_2](H_2O)$ [62] (c).

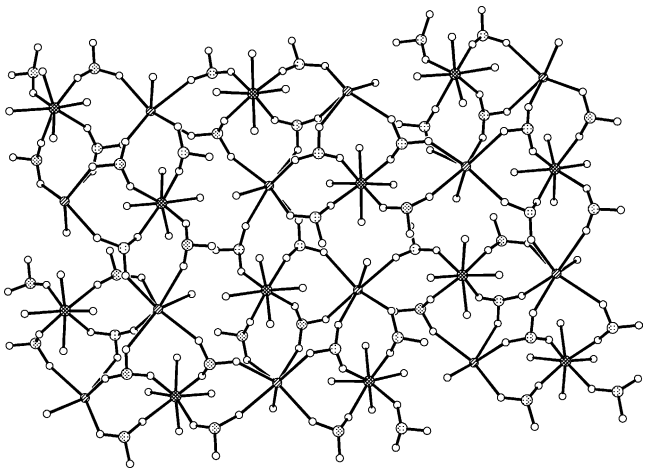

Fig. 6. The inorganic metal–sulfonate layer in $[K(OH_2)_2Yb(OH_2)_4\{o\text{-}C_6H_4(SO_3)_2\}_2]_n$ [66].

or *anti* coordination conformation adopted by the sulfonate oxygen.

1.3. Functional metal sulfonates

Materials with absorption properties have attracted much attention due to their potential applications in chemical storage, separation and catalysis. There are two major categories of metal-containing absorptive materials, namely the well-studied zeolites with rigid and stable frameworks which are mostly not sensitive to guest uptaking [69,70], and the microporous coordination metal complexes with supramolecular frameworks [71–73]. Metal coordination frameworks, with more flexibility in comparison with that of zeolites, can be designed and modified adequately via using different type of metal centers and functional groups [74]. Among them, rigid functional groups, such as phosphates [4,75], carboxylate [76,77], bipyridine [70], or a mixture of both carboxylate and bipyridine ligands [78–80] have been employed to construct porous frameworks with high dimensionalities. However, this approach has been challenged by two major hindrances. One is the interpenetration of the framework when forming higher dimensional structures, thus prohibiting the formation of the pores. Another one is that removal of the guest molecules could cause the frameworks to collapse irreversibly. Only very recently, by employing large and rigid metal carboxylate clusters as secondary building units for host design, have the problems of interpenetration and framework fragility of porous metal organic frameworks been circumvented [81,82].

Water-coordinated metal phosphonates with inorganic–organic lamellar structures have been studied extensively and they represent another type of absorbing metal organic materials [83–89]. These compounds can intercalate amines after excluding the coordinated water molecules from the coordination sites of the metal center. The resulting intercalatants are stable since coordinative bonds are formed between amines and the metal centers. On the other hand, the intercalation or adsorption behavior of metal sulfonates were reported [7,90–94] and reviewed recently by Côté and Shimizu [1]. Silver triflate could uptake alcohol via a topotactic process [91], while silver 3-pyridinesulfonate displays selective MeCN uptake which triggers a phase transition in solid state [90]. In both cases, the intercalation behavior is contributed by the flexible coordination modes of Ag^+ with sulfonate groups. Furthermore, in the preliminary experiment [7], it was shown that layered metal sulfonate compound AgOTs can intercalate nonylamine when it is treated with the liquid amine. However, no detailed structural analyses were conducted to elucidate the intercalation process and identify the structure of the resulting complex.

1.4. Scope of this review and abbreviations

Owing to the weak coordination strength of $-SO_3^-$, most sulfonate ions cannot efficiently displace solvents from the primary coordination sphere of the transition metal ions [1]. For instance, in the effort to generate the structural analogs of metal phosphonates, metal benzenesulfonate and naphthalenesulfonate salts were synthesized [95–99]. Nevertheless, in most metal sulfonates obtained from aqueous solution, the metal ions are hydrated to a great extent. Especially, all the transition metal sulfonates involve segregation

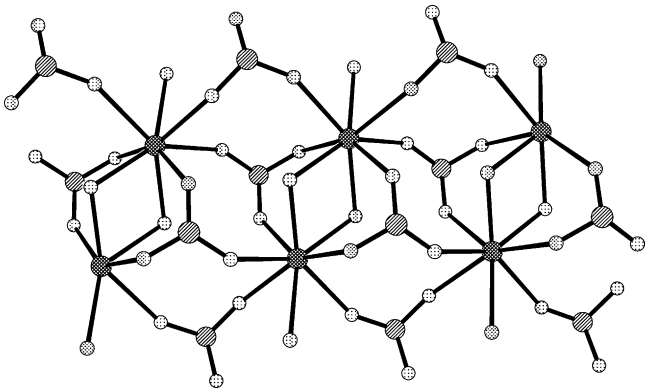

Fig. 7. The inorganic metal–sulfonate layer in $\{Ln(OH)(1,5nds)(H_2O)\}_n$ (Ln = La, Pr and Nd) [68].

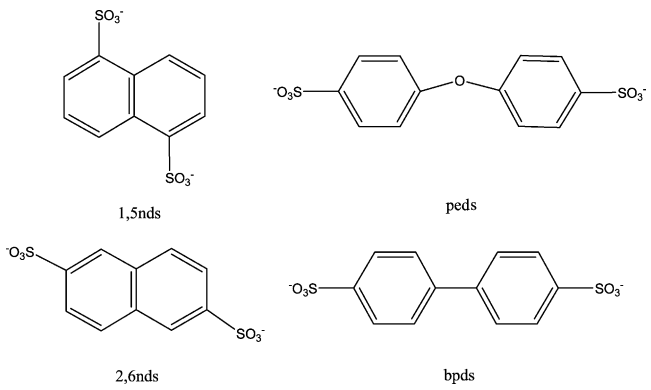

Fig. 8. Arenedisulfonate ligands used in this study.

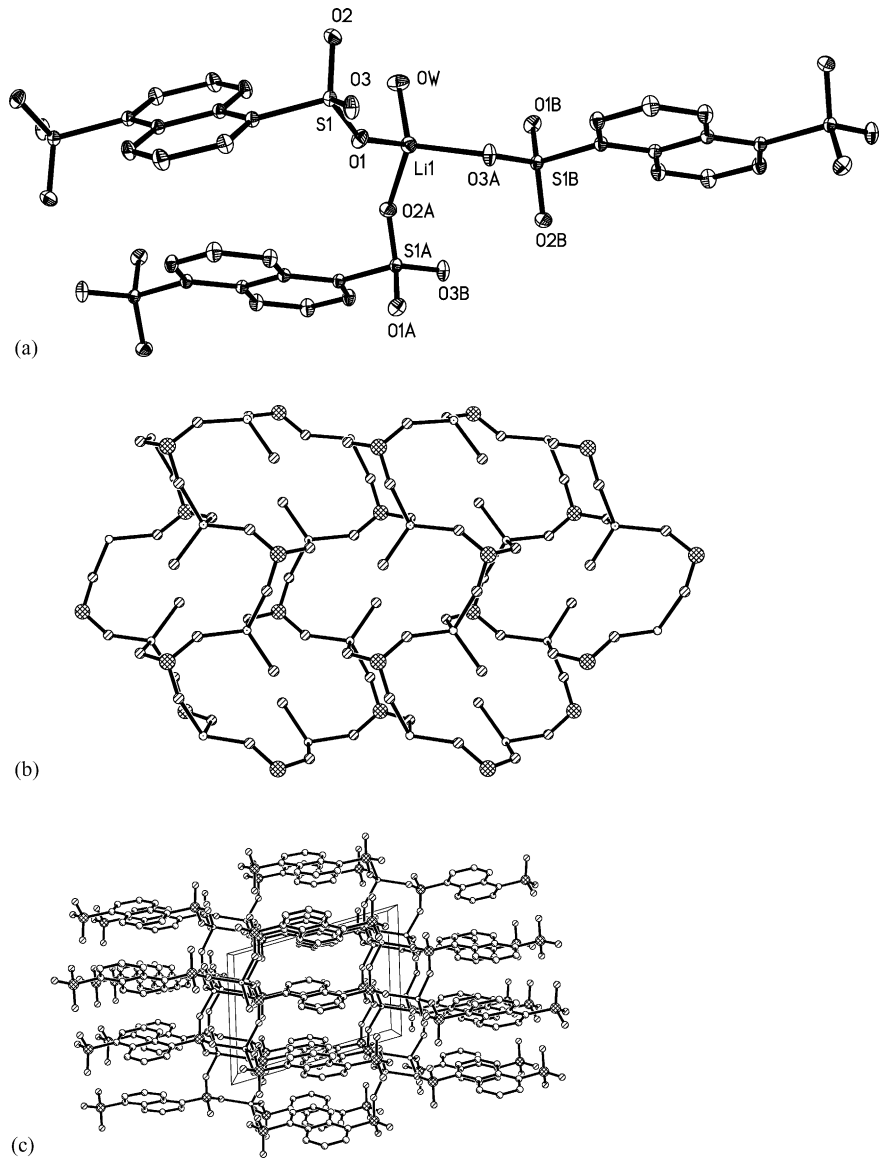

Fig. 9. Coordination environment of Li^+ (a), the inorganic metal–sulfonate layer (b) and packing in $[Li_2(1,5nds)(H_2O)_2]_n$.

of the aquametal complex cations and sulfonate anions without any direct metal–sulfonate interactions [97–99]. In the case of the alkali metals [95,96], larger alkaline earth metals [98,99], silver [1] and the rare-earth metal ions [66], the metal ions could be coordinated by both aqua molecules and sulfonate oxygen.

In this review, we will demonstrate that by employing disulfonates to provide multiple coordination sites and amines as auxiliary ligands, stable main group and transition metal sulfonates can be obtained from aqueous solution with frameworks sustained or dominated by metal–sulfonate interactions [5,100–104]. Furthermore, the results obtained in our group concerning the systematic investigation of the amine uptake properties of two water-coordinated layered metal sulfonates will also be outlined [105,106].

The following abbreviations will be used throughout in this paper. The disulfonates ligands used for this study are shown in Fig. 8. 1,5nds = 1,5-naphthalenedisulfonate; 2,6nds = 2,6-naphthalendisulfonate; bpds = 4,4′-biphenyldisulfonate; peds = 4,4′-phenyletherdisulfonate; en = ethylenediamine; *N*-meen = *N*-methylethylenediamine; dpn = 2,3-diaminopropane; tren = tris(2-aminoethyl)amine; *N*,*N*′-meen = *N*,*N*′-dimethylethylenediamine; dien = diethylenetriamine; cyclam = 1,4,8,11-tetraazacyclotetradecane; 2,2′-bpy = 2,2′-bipyridyl; inia = isonicotinamide.

2. Structures of metal arenedisulfonates

2.1. Main group metals

Six solid-state structures of alkali and alkaline earth metal 1,5-naphthalenedisulfonates [5] as well as Na_2(peds)

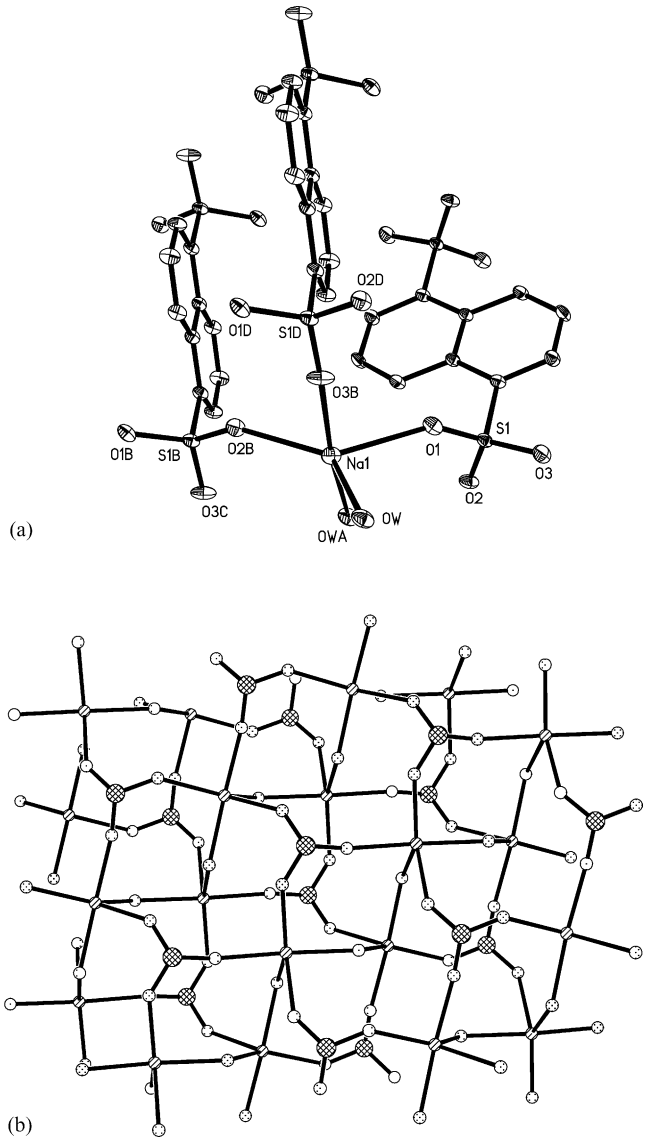

Fig. 10. Coordination environment of Na^+ (a) and the metal–sulfonate layer (b) in $[Na_2(1,5nds)(H_2O)_2]_n$.

[6] were investigated. All the three alkali compounds $[M_2(1,5nds)(H_2O)_2]_n$ (M = Li^+, Na^+, K^+) crystallize in the same space group $P2_1/c$ with different unit cell parameters. Despite the difference in the coordination behavior of the metal ions, their packing arrangements are very similar and only the Li^+ analog is shown in Fig. 9c. Interestingly, all three analogs adopt 3D frameworks constructed by inorganic–organic layers, with the metal–sulfonate inorganic portions pillared by the naphthalene rings, reminiscent of the reported metal biphosphonate compounds [107].

As shown in Fig. 9a, Li^+ is coordinated by one water molecule and three different $–SO_3^-$ groups. Every $–SO_3^-$ oxygen atom is coordinated to one Li^+ and the $–SO_3^-$ group functions as a $\eta^3\ \mu^3$ bridge, connecting three Li^+ ions with Li–O = 1.919(3)–1.994(3) Å, as showed in Fig. 9b. While Na^+ is 5-coordinated by three different $–SO_3^-$ groups and

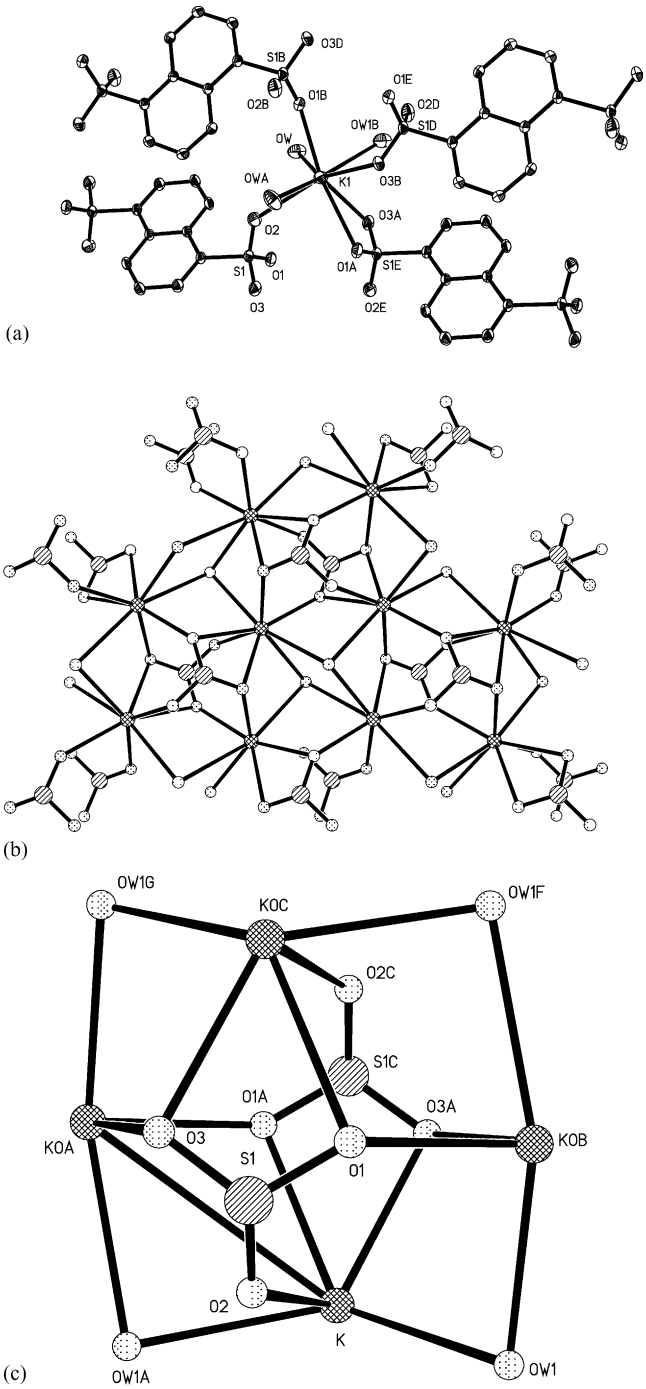

Fig. 11. Coordination environment of K^+ (a), the metal–sulfonate layer (b) and the unique cage structure constructed by two μ_4 $–SO_3^-$ groups, four potassium ions and four water molecules (c) in $[K_2(1,5nds)(H_2O)_2]_n$.

two water molecules, as shown in Fig. 10a. Every $–SO_3^-$ oxygen is coordinated to one Na^+ ion and the $–SO_3^-$ group functions as a $\eta^3\ \mu^3$ bridge connecting three Na^+ ions, with Na–O = 2.3185(12)–2.3567(13) Å, as indicated in Fig. 10b. The K^+ ion is 8-coordinated by three water molecules and five $–SO_3^-$ oxygen atoms from four different groups, as shown in Fig. 11a, with K–O = 2.6693(15)–2.8751(15) Å. Two of the $–SO_3^-$ oxygen atoms (O1 and O3) are coordinated to

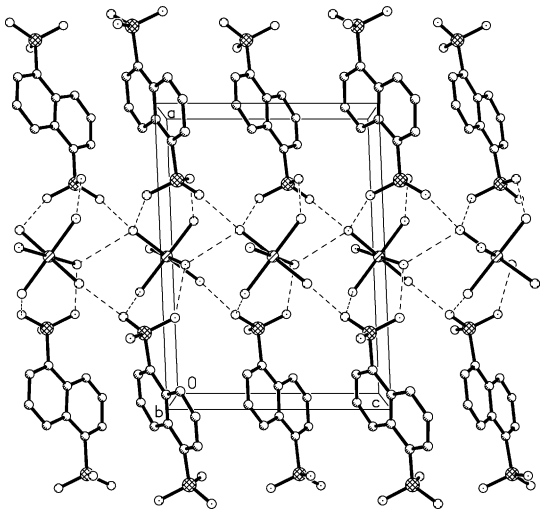

Fig. 12. The packing structure of $[Mg(H_2O)_6]$ (1,5nds).

two K^+ ions, which make the $–SO_3^-$ group function as a η^5 μ^4 bridge. In the mean time, the K^+ ion is coordinated by two oxygen atoms from the same $–SO_3^-$ group, as shown in Fig. 11b and c.

The corresponding characteristic O–H stretching and S–O vibrational frequencies in their IR spectra also clearly indicate the different coordination behavior of the sulfonate groups. Despite the different coordination structure of the metal ions, the Li^+, Na^+ and K^+ analogs crystallize with the same cell component and space group. The increasing coordination strength with decreasing charge–radius ratio is illustrated adequately in these three alkali metal ion structures.

There is no direct coordination of Mg^{2+} by sulfonate in the magnesium(II) analog, $[Mg(H_2O)_6]$(1,5nds). The Mg^{2+} ion is coordinated by six water molecules while the sulfonate groups behave as counter-anions forming extensive hydrogen bonding interactions with the aquametal complexes, as shown in Fig. 12. In the calcium(II) analog $[Ca(1,5nds)(H_2O)_2]_n$, Ca^{2+} is octahedrally coordinated by four $–SO_3^-$ groups which construct the basal plane with Ca–O = 2.3043(12)–2.3754(12) Å, and two water molecules in the axial positions, with distances of 2.3182(13) and 2.3327(13) Å, respectively. Each $–SO_3^-$ behaves as a η^2 μ^2 ligand bridging two Ca^{2+} ions, thus constructing a 2D network with alternating organic–inorganic components, as shown in Fig. 13.

As shown in Fig. 14a, the strontium(II) analog $[Sr(1,5nds)(H_2O)_2]_n$, Sr^{2+} is 8-coordinated to six different $–SO_3^-$ groups, with Sr–O = 2.5190(14)–2.5531(14) Å, and two water molecules with distances of 2.692(2) and 3.014(3) Å, respectively. Each of the $–SO_3^-$ oxygen is coordinated to different Sr^{2+}, resulting in a η^3 μ^3 bridging mode similar to that adopted by Li^+ and Na^+. The inorganic layer structure is shown in Fig. 14b. All the Sr^{2+} ions locate on the same least-square plane. Three Sr^{2+} ions are bridged together by two μ^3 $–SO_3^-$ groups below and above the square plane. As shown in Fig. 14c, $[Sr(1,5nds)(H_2O)_2]_n$ is a 3D structure similar to that adopted by the alkali metal analogs. The Ba^{2+} analog is an isostructure of $[Sr(1,5nds)(H_2O)_2]_n$, with Ba–O = 2.6696(18)–2.7232(18) Å.

With the decrease of charge–radius ratio, the coordination strength of alkali metal ion increases in the order $Li^+ < Na^+ < K^+$, as illustrated nicely by the coordination number of 4, 5 and 8 for the Li^+, Na^+ and K^+ analogs. Even though in the Li^+, Na^+, Sr^{2+} and Ba^{2+} analogs, the $–SO_3^-$ groups adopt the same η^3 μ^3 bridging mode and the overall packing arrangements are the same inorganic–organic lamellar, different inorganic layer structures are observed. The discrepancy is contributed by the different coordination properties of the metal ions.

Finally, in $[Na_2(peds)]_n$, the Na^+ ion is 7-coordinated by five different $–SO_3^-$ groups, as shown in Fig. 15a, with Na–O = 2.3183(17)–2.6015(19) Å. Two of the oxygen atoms are involved with two Na^+ ions. The third oxygen atom

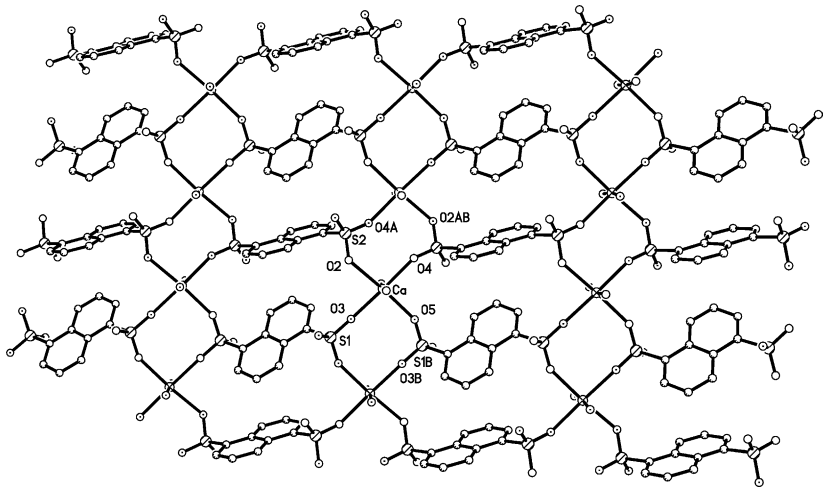

Fig. 13. The layered structure of $[Ca(1,5nds)(H_2O)_2]_n$.

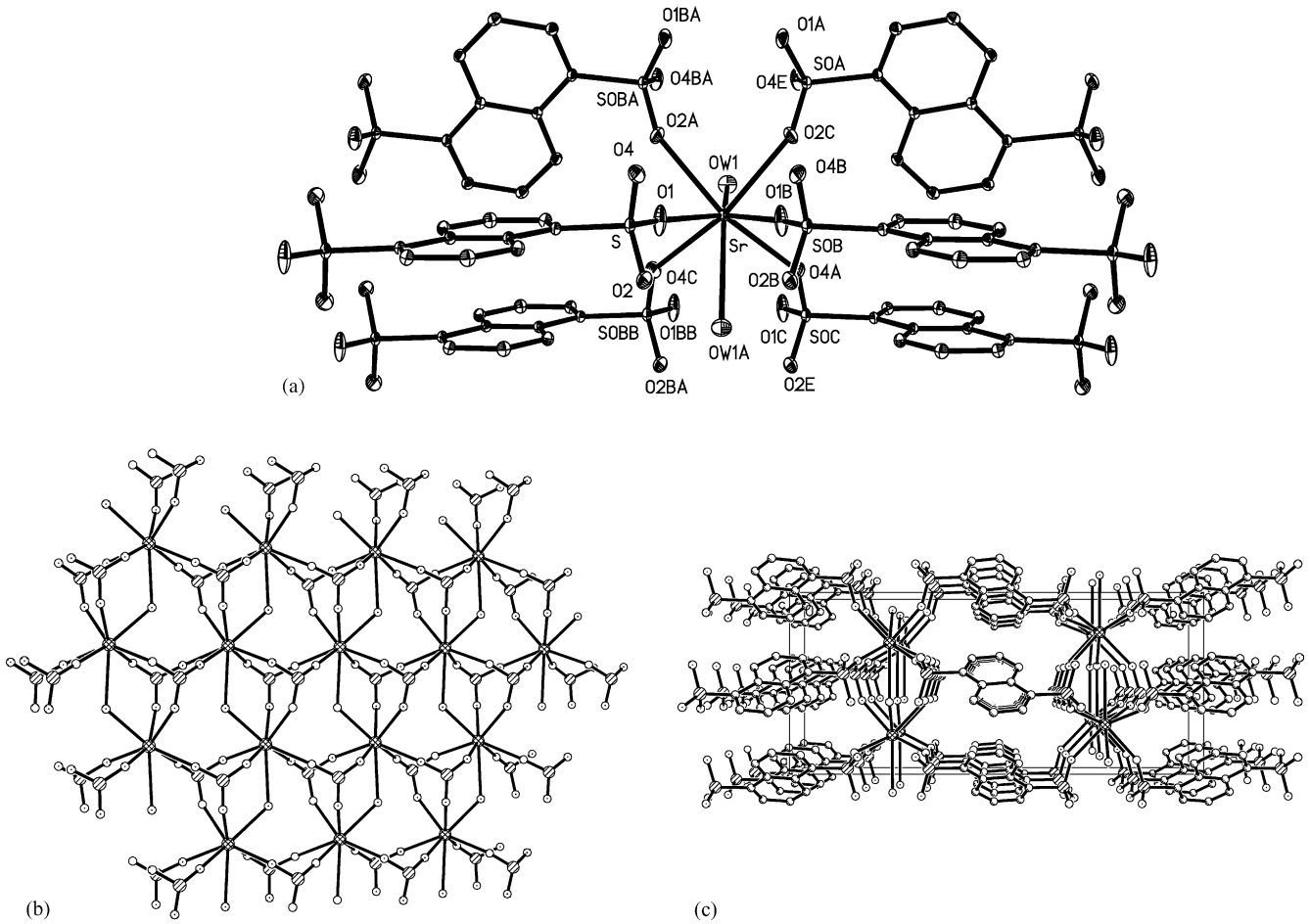

Fig. 14. Coordination environment of Sr^{2+} (a), 2D metal–sulfonate layer (b) and 3D structure (c) of $[Sr(1,5nds)H_2O]_n$.

is coordinated by three Na^+ ions, with two of them sharing the other oxygen atoms, resulting in an unusual η^7 μ^5 coordination mode for the sulfonate group, as shown in Fig. 15b. The 3D framework is similar to that observed in $[Na_2(1,5nds)(H_2O)_2]_n$. However, the coordination modes of the sulfonate group have been changed dramatically from η^3 μ^3 in $[Na_2(1,5nds)(H_2O)_2]_n$ to η^7 μ^5 in $[Na_2(peds)]_n$. It is noted that peds is a ligand with a flexible backbone in contrast to the rigid naphthalene ring carried by the 1,5nds ligand. Therefore, the two $–SO_3^-$ groups of the peds ligand can adjust themselves to better accommodate the Na^+ ions. The stark difference in the coordination modes of the sulfonate groups observed in $[Na_2(1,5nds)(H_2O)_2]_n$ and $[Na_2(peds)]_n$ demonstrates vividly the flexibility of the sulfonate coordination modes.

2.2. Transition metals

$[Cd(1,5nds)(H_2O)_2]_n$ is a 2D layered compound which adopts the same arrangement as that of $[Ca(1,5nds)(H_2O)_2]_n$ [5,102]. The Cd^{2+} ion is coordinated by four $–SO_3^-$ groups, with Cd–O = 2.250(3)–2.342(2) Å, and two water molecules. Each $–SO_3^-$ group behaves as a η^2 μ^2 ligand bridging two Cd^{2+} ions, constructing a 2D network with alternating organic–inorganic components, as shown in Fig. 16a. In contrast to the 1,5-naphthalenedisulfonate salts of the alkali and alkaline earth metals described above, which all crystallize in the centro-symmetric space group with the 1,5nds ions sitting on the inversion centers, there is one 1,5nds ion located on a general position, and two 1,5nds located on the inversion centers in $[Cd(1,5nds)(H_2O)_2]_n$, thus resulting in four independent $–SO_3^-$ groups in the asymmetric unit with slightly different bonding distance to Cd^{2+}. Consequently, the inorganic layer consists of three differently conformed 8-membered rings, with Cd···Cd separations of 5.472, 5.195 and 5.53 Å, respectively. This structural feature indicates that the 2D cadmium(II) sulfonate network directed by the 8-membered rings is flexible and elastic, which could endure some structural contraction or expansion. Strong inter-layered hydrogen bonding interactions formed between the coordinated water molecules and the free $–SO_3^-$ oxygen atoms extend the layers into a 3D network, as shown in Fig. 16b.

Interestingly, the 3D polymorph of the 2D $[Cd(1,5nds)(H_2O)_2]_n$ compound is also obtained, which crystallizes in a different space group with different

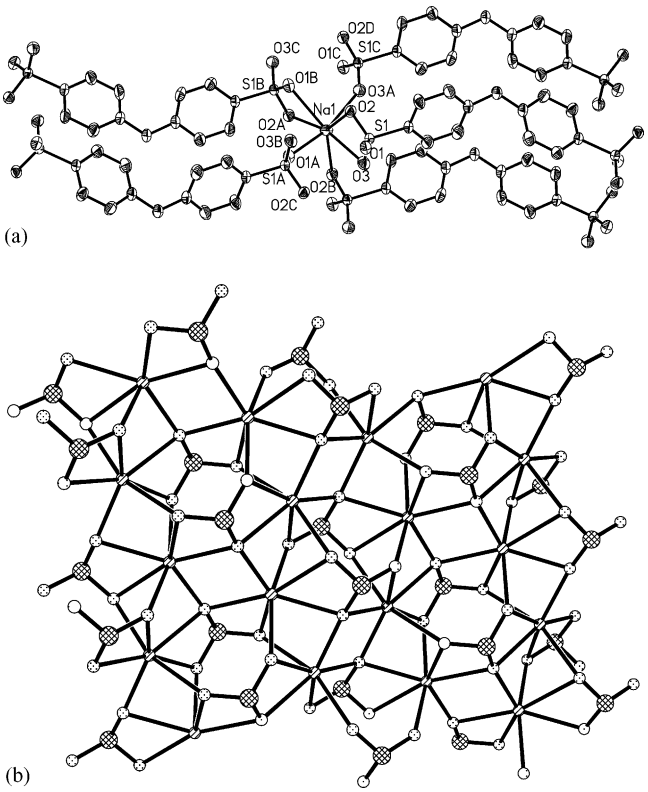

Fig. 15. The coordination structure of Na^+ (a) and the 2D metal–sulfonate layer (b) in $[Na_2(peds)]_n$.

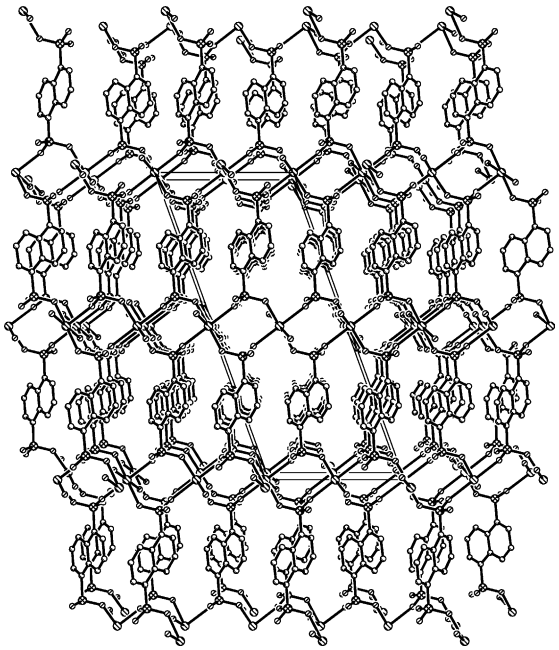

Fig. 17. The 3D polymorph of $[Cd(1,5nds)(H_2O)_2]_n$.

arrangement [108]. Both the Cd^{2+} and 1,5nds ions are located on the inversion centers and there is only one independent $-SO_3^-$ group present in the asymmetric unit. In these two polymorphs, the coordination geometries around the Cd^{2+} ions as well as the coordination modes of the 1,5nds ions are the same. However, the 1,5nds anions connect Cd^{2+} ions belonging to different layers, thus resulting in a 3D framework

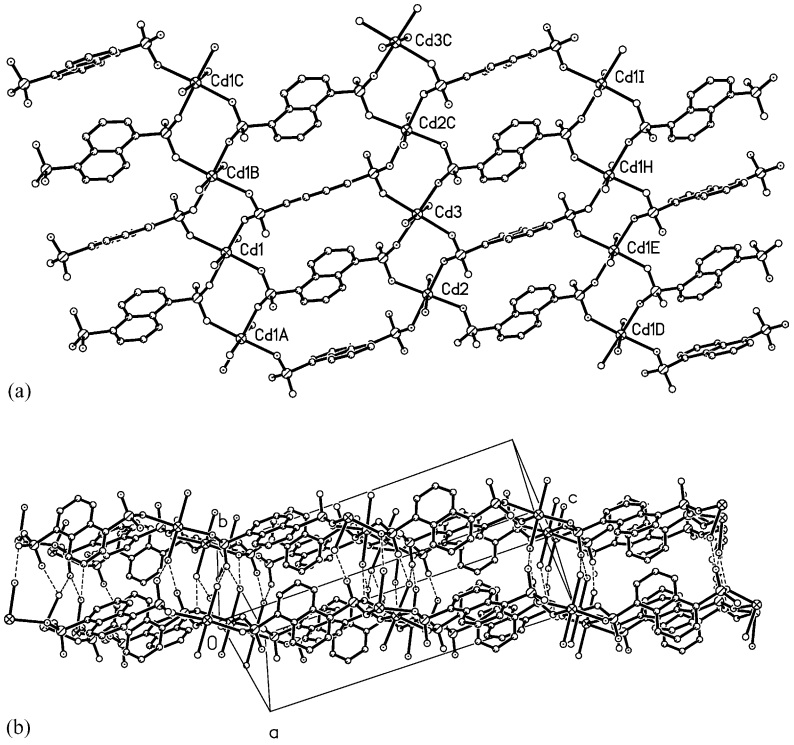

Fig. 16. The 2D layered polymorph of $[Cd(1,5nds)(H_2O)_2]_n$ (a) and the packing showing inter-layered hydrogen bonds (b).

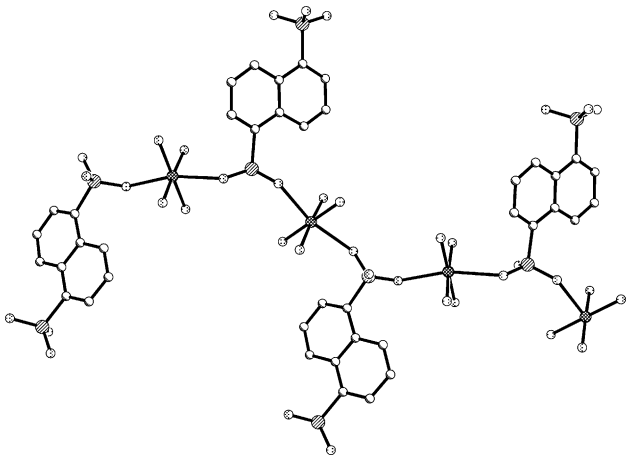

Fig. 18. The 1D chain formed by $[Cu(H_2O)_4(1,5ndsH)]_n$.

similar to that observed in the alkali and alkaline earth metal analogs, as shown in Fig. 17.

Copper(II) 1,5-naphthelenedisulfonate is isolated from aqueous solution and identified as $[Cu(H_2O)_6](1,5nds)$. In contrast, when copper(I) salt is used, $[Cu(H_2O)_4(1,5ndsH)]_n$ is obtained [108], in which one $–SO_3^-$ group is protonated, while the other $–SO_3^-$ group coordinates to two different $[Cu(H_2O)_4]^+$ ions in *syn–anti* fashion, resulting in a 1D structure shown in Fig. 18, with Cu–O = 2.337 and 2.449 Å for the coordinated sulfonate group. The 1D chains are linked via extensive hydrogen bonds formed between the free $–SO_3H$ groups and the coordinated water molecules.

3. Structures of complexes with mixed-ligand of arenedisulfonates and amines

According to what we have observed and those documented by CSD, the maximum number of coordination sites provided by each sulfonate group to the divalent transition metal ion observed so far is 2. Therefore, leaving out the *syn–anti* conformational variable, there are six possible coordination modes provided by a μ^2-coordinated disulfonate ion, as shown in Fig. 19. All these six possible coordination modes are adopted by the arenedisulfonates in Cu^{2+} and Cd^{2+} complexes under different chemical environments. For instance, mode (a) is found in $[Cd(2,2'\text{-bpy})_2(H_2O)(peds)]\cdot 4H_2O$, mode (b) in $[Cd(cyclam)(1,5nds)]_2$, mode (c) in $\{[Cu(en)_2(1,5nds)]\cdot 2H_2O\}_n$ and $[Cu(dpn)_2(bpds)]_n$, mode (d) in $[Cd_2(2,2'\text{-bpy})_4(H_2O)_2(1,5nds)](1,5nds)\cdot 4H_2O$, $\{[Cd(inia)_2(H_2O)_2(2,6nds)]\cdot 4H_2O\}_n$, $\{[Cd(inia)_2(H_2O)_2(bpds)]\cdot 4H_2O\}_n$ and all the 1D polymers described in Section 3.2, mode (e) in $\{[Cd_2(inia)_4(H_2O)_3(peds)_2]\cdot 2H_2O\}_n$, and mode (f) in $[Cd(1,5nds)(H_2O)_2]_n$. Among them, the centrosymmetric trans μ^2 bridging mode (d) is most frequently adopted.

3.1. Cu^{2+} complexes

The solid-state structures of $\{[Cu(en)_2(1,5nds)]\cdot 2H_2O\}_n$, $\{[Cu(N\text{-meen})_2(2,6nds)]\cdot H_2O\}_n$, $[Cu(dpn)_2(bpds)]_n$, $[Cu(cyclam)(1,5nds)]_n$, $[Cu(dpn)_2(H_2O)_2](1,5nds)$ and $[Cu(N,N'\text{-meen})_2(H_2O)_2](1,5nds)\cdot H_2O$, together with $[Cu(H_2O)_6](1,5nds)$ [100] demonstrate that the coordination behavior of Cu^{2+} toward $–SO_3^-$ can be tailored chemically, and that the arenedisulfonate ion can compete with water molecules and coordinate with Cu^{2+}. On the other hand, the interaction between Cu^{2+} and sulfonate is weak and sensitive to trivial modification of the chemical and geometrical environment.

All the amine-containing complexes have similar components, and the Cu^{2+} ions have the same CuN_4O_2 chromophore, 6-coordinated equatorially by four nitrogen atoms from the amine ligands and axially by two oxygen atoms from two $–SO_3^-$ groups or two water molecules. The CuN_4O_2 chromophores are tetragonally elongated to different extent along the axial positions. All the CuN_4O_2 chromophores are centrosymmetric except for $\{[Cu(en)_2(1,5nds)]\cdot 2H_2O\}_n$, which crystallizes in an enantiomorphic space group $P4_12_12$. In $\{[Cu(en)_2(1,5nds)]\cdot 2H_2O\}_n$, $\{[Cu(N\text{-meen})_2$

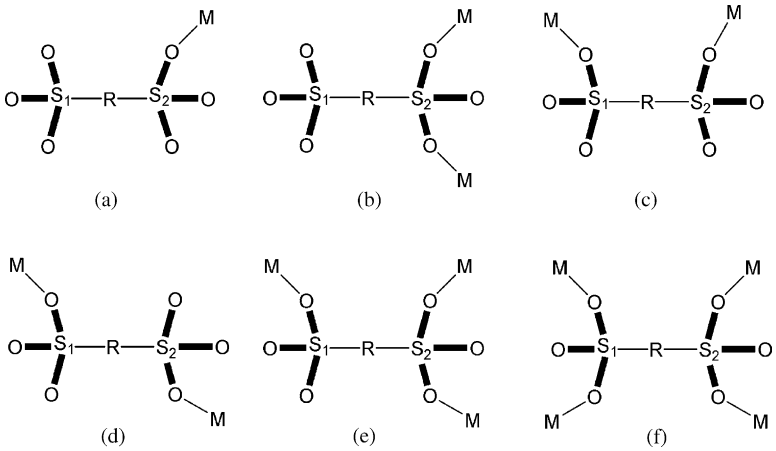

Fig. 19. Schematic representation of the six possible coordination modes of the disulfonate anions, if each $–SO_3^-$ group could be monodentate or μ^2 bridging.

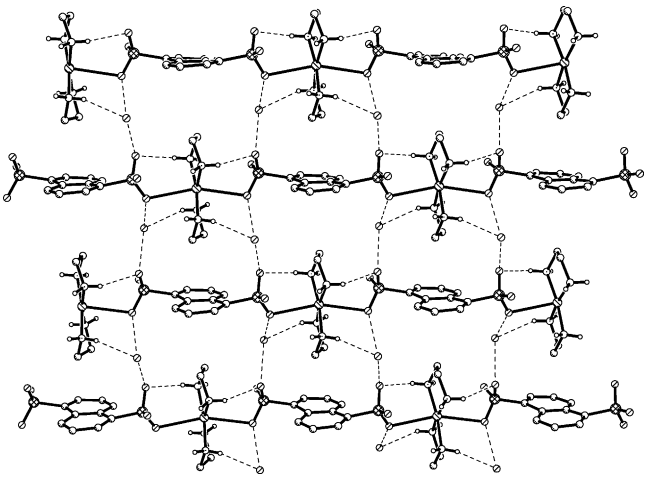

Fig. 20. The extended 2D layer observed in $\{[Cu(en)_2(1,5nds)]\cdot 2H_2O\}_n$.

$(2,6nds)]\cdot H_2O\}_n$, $[Cu(dpn)_2(bpds)]_n$ and [Cu(cyclam)(1,5nds)]$_n$, each $-SO_3^-$ coordinates monodentately to Cu^{2+}, and the naphthalenedisulfonate and biphenyldisulfonate ions behave as bifunctional spacers, bringing the complex cations into infinite 1D strings, as shown in Figs. 20–23.

Two parameters are adopted to describe and compare the coordination geometries of this series of compounds. θ_1 is the torsion angle of C–S–O–Cu for the coordinated sulfonate oxygen, and θ_2 the dihedral angle formed between the equatorial planes of $[CuN_4]$ and the naphthalene or phenyl rings. The scattering distribution of these parameters reveals the diverse geometries similar to that observed in the coordination behavior of zirconium arenesulfonates [58]. The aromatic rings and the equatorial planes of the Cu^{2+} complex cations tend to be perpendicular to each other in $\{[Cu(en)_2(1,5nds)]\cdot 2H_2O\}_n$ and [Cu(cyclam)(1,5nds)]$_n$. While $\{[Cu(N\text{-meen})_2(2,6nds)]\cdot H_2O\}_n$ and $[Cu(dpn)_2(bpds)]_n$ display another coordination geometry, in which the C–S and Cu–O bonds are close to be perpendicular to each other and the two least-squares planes of the cation and anion tend to be coplanar. There is a relation between the collinearity of the Cu–O–S–C fragments and the coplanarity of the two least-squares planes of the cation and anion. The homogeneity of the torsion angles of C–S–O2–Cu and C–S–O3–Cu (O2 and O3 are the non-coordinated sulfonate oxygen atoms) observed in

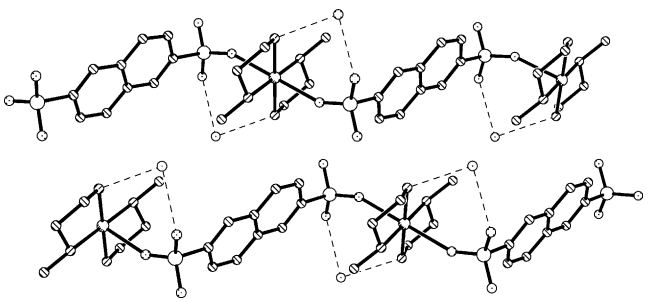

Fig. 21. $\{[Cu(N\text{-meen})_2(2,6nds)]\cdot H_2O\}_n$.

$\{[Cu(en)_2(1,5nds)]\cdot 2H_2O\}_n$ and [Cu(cyclam)(1,5nds)]$_n$ is consistent with a closer approach of $-SO_3^-$ oxygen toward the Cu^{2+} core in order to facilitate hydrogen bonding interactions with the amine ligands coordinated to the metal ion. The different geometries of the coordination sphere, as well as the free rotation about the S–C bond, produce diverse topologies for the 1D chains. In $\{[Cu(en)_2(1,5nds)]\cdot 2H_2O\}_n$ and [Cu(cyclam)(1,5nds)]$_n$, the chains are almost linear, as indicated by the θ_1 value close to 180°. $\{[Cu(N\text{-meen})_2(2,6nds)]\cdot H_2O\}_n$ forms a wave-like structure. While in $[Cu(dpn)_2(bpds)]_n$, the serrated profile of a castellation is formed. The conformational freedom engenders various topologies, and such a phenomenon is structurally less predictable and explored in coordination polymers, as compared with the predictable architectures employing linear and rigid linking groups, such as 4,4′-bipyridine.

In complexes $[Cu(dpn)_2(H_2O)_2](1,5nds)$ and $[Cu(N,N'\text{-meen})_2(H_2O)_2](1,5nds)\cdot H_2O$, the Cu^{2+} ions are coordinated by water molecules, instead of the sulfonate oxygen atoms, as shown in Figs. 24 and 25. Steric hindrance, caused by the C- or N-substitution of the amine ligands, could be responsible for preventing the effective approach of the bulky $-SO_3^-$ group to Cu^{2+}. Compounds $[Cu(dpn)_2(bpds)]_n$ and $[Cu(dpn)_2(H_2O)_2](1,5nds)$ have the same $[Cu(dpn)_2]^{2+}$ square cation. However, with the C–C bond capable of rotation, the bpds ligand is much more flexible than the 1,5nds ligand to promote better metal–sulfonate interaction.

3.2. 1D Cd^{2+} complexes

Four Cd^{2+} arenedisulfonate polymers, namely $[Cd(N,N'\text{-meen})_2(2,6nds)]_n$, $[Cd(N,N'\text{-meen})_2(1,5nds)]_n$, $[Cd(N,N'\text{-meen})_2(bpds)]_n$, and $\{[Cd(N\text{-meen})_2(2,6nds)]\cdot 2H_2O\}_n$, were synthesized in aqueous solution and structurally characterized by X-ray single-crystal diffraction [101]. Their structures are shown in Figs. 26–29. In all these four structures, Cd^{2+} is 6-coordinated equatorially by four nitrogen atoms from the amine ligands and axially by two oxygen atoms from the monodentate $-SO_3^-$ groups. The Cd–O distances are in the range of 2.3504(19)–2.4324(13) Å. The arenedisulfonate anions act as bifunctional spacers to coordinate the CdN_4 complex cations, generating stepwise 1D strings. In contrast to the Cu^{2+} analogs, the coordination conformations of the sulfonate groups vary to a much smaller extent. This observation is in line with the similar stepwise 1D structures observed in all the four compounds.

Due to the inherent multiple H-bonding donors/acceptors on their neutral polymeric backbones, the same pattern of inter-chain hydrogen bonding interactions described as $C(6)R_2^2(12)$ are formed by the amino hydrogen atoms and sulfonate oxygen atoms, despite the differences in both the ligands and space groups. The four polymers arrange in a very similar pattern of extended 2D networks, as illustrated in Fig. 30. Hence, a unique supramolecular synthon formed by direct hydrogen bonding interactions between two 1D

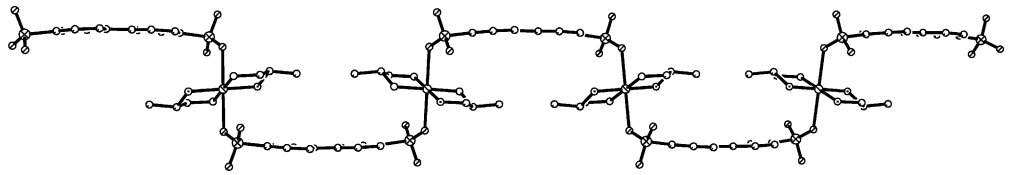

Fig. 22. $[Cu(dpn)_2(bpds)]_n$.

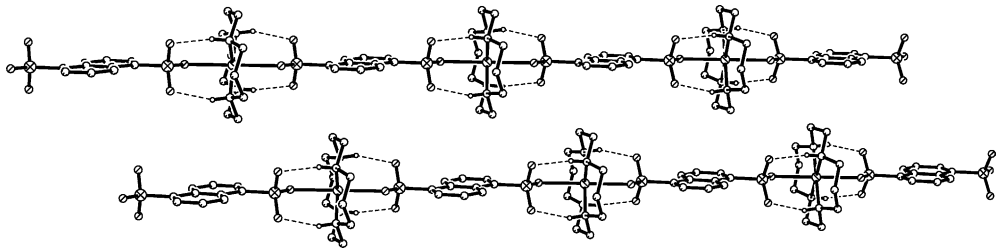

Fig. 23. $[Cu(cyclam)(1,5nds)]_n$.

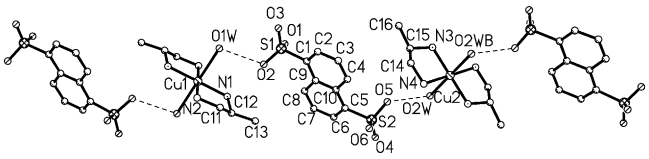

Fig. 24. $[Cu(dpn)_2(H_2O)_2](1,5nds)$.

polymeric backbones, as the driving force for the assembly of these 1D polymers into 2D networks, has been rationalized.

Despite the differences in the coordination geometries in $\{[Cu(N\text{-meen})_2(2,6nds)]\cdot 2H_2O\}_n$ and $\{[Cd(N\text{-meen})_2(2,6nds)]\cdot 2H_2O\}_n$ (elongated versus regular octahedral MN_4O_2 chromophores, Cu–N = 2.029(2) and 2.068(2) Å, Cu–O = 2.496(2) Å versus Cd–N = 2.2961(18) and 2.3497(18) Å, Cd–O = 2.4245(15) Å), they are isostructural. The packing arrangements of these two compounds are very similar. The inter-chain hydrogen bonding strength is weaker in the Cu^{2+} analog (N···O 3.142(4) Å, N–H···O 134.6° versus N···O 3.078(2) Å, N–H···O 144.2°). Finally, the 2D array illustrated in Fig. 30 is only observed in polymers with stepwise or wave-like topology. For the linear $\{[Cu(en)_2(1,5nds)]\cdot 2H_2O\}_n$, and $[Cu(cyclam)(1,5nds)]_n$, and the castellated $\{[Cu(dpn)_2(bpds)]\cdot H_2O\}_n$, different arrangements are adopted.

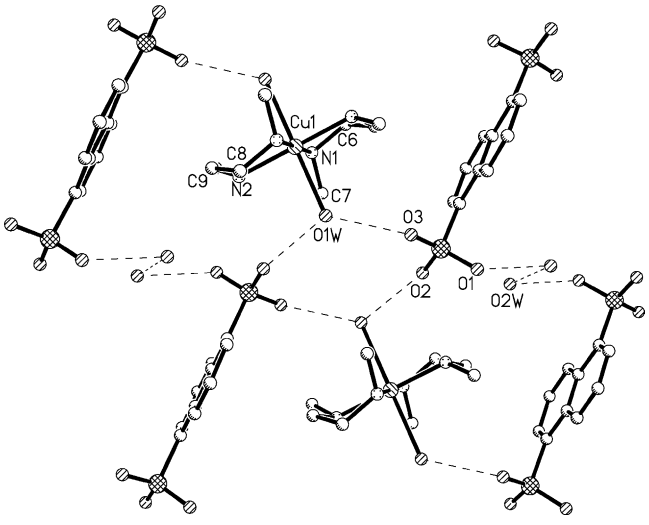

Fig. 25. $[Cu(N,N'\text{-meen})_2(H_2O)_2](1,5nds)\cdot H_2O$.

The most significant feature about the synthon observed in the Cd^{2+} analogs is the flexibility. Even though the inter-chain H-bonding pattern $C(6)R_2^2(12)$ is persistent in all the structures studied here and also in the Cu^{2+} analog of $[Cd(N\text{-meen})_2(2,6nds)]\cdot 2H_2O$, it is elastic enough to adapt to certain variations introduced by different coordination modes of the disulfonate toward the metal center, the nature of the organic group (naphthalene versus biphenyldisulfonate) and the amino ligand (*N*,*N*′-meen versus *N*-meen), clathration of water molecules, as well as different metal ions with the same charge.

3.3. Cd^{2+} complexes with diverse disulfonate coordination modes

Six mono- and dinuclear cadmium(II) arenedisulfonate compounds with zero- or one-dimensional architecture, namely $[Cd(2,2'\text{-bpy})_2(H_2O)(peds)]\cdot 4H_2O$, $[Cd_2(2,2'\text{-bpy})_4(H_2O)_2(1,5nds)](1,5nds)\cdot 4H_2O$, $[Cd(cyclam)(1,5nds)]_2$, $\{[Cd(inia)_2(H_2O)_2(2,6nds)]\cdot 4H_2O\}_n$, $\{[Cd(inia)_2(H_2O)_2(bpds)]\cdot 4H_2O\}_n$, and $\{[Cd_2(inia)_4(H_2O)_3(peds)_2]\cdot 2H_2O\}_n$, were obtained from aqueous solution using similar procedures and structurally characterized by X-ray single-crystal diffraction [102].

The Cd^{2+} ions in all compounds are 6-coordinate with octahedral geometry distorted to varying degrees. The distances between Cd^{2+} and the coordinated sulfonate oxygen (∼2.3 Å) are very consistent. Both the *syn* and *anti* coordination modes of the metal sulfonate fragments

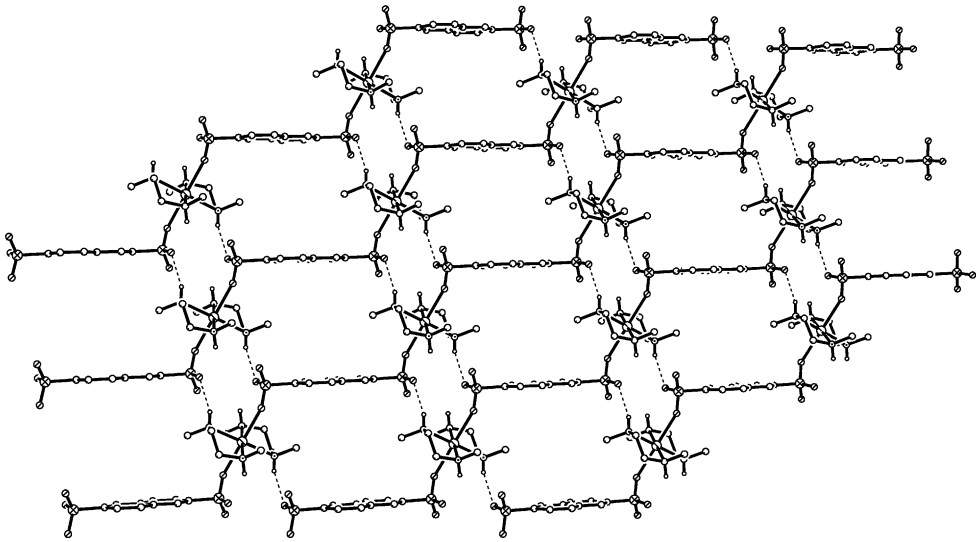

Fig. 26. $[Cd(N,N'\text{-meen})_2(2,6nds)]_n$.

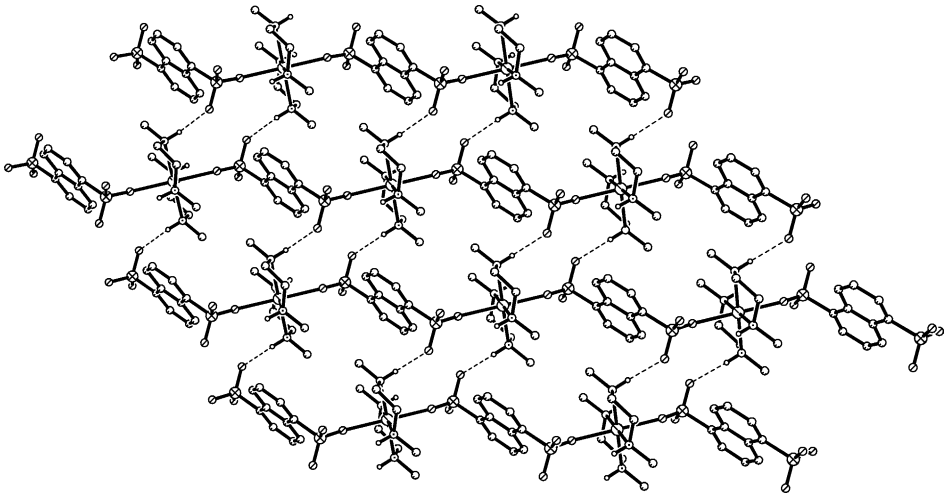

Fig. 27. $[Cd(N,N'\text{-meen})_2(1,5nds)]_n$.

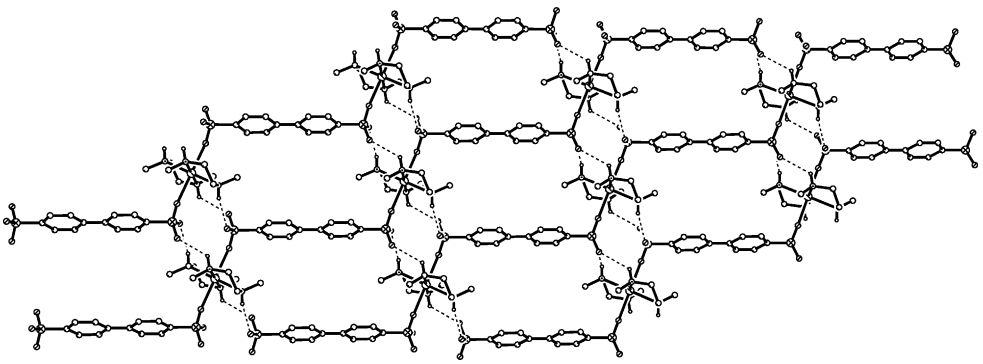

Fig. 28. $[Cd(N,N'\text{-meen})_2(bpds)]_n$.

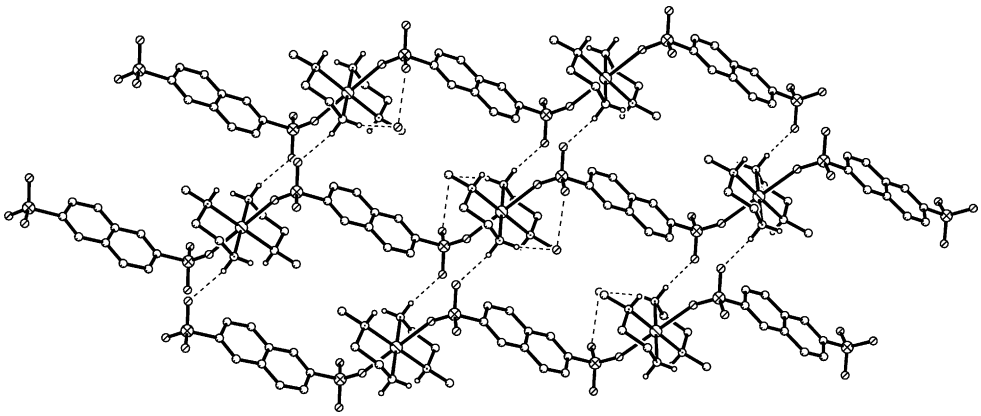

Fig. 29. $\{[Cd(N\text{-meen})_2(2,6nds)]\cdot 2H_2O\}_n$.

are observed. The most diverse geometrical parameter around the Cd^{2+} coordination core is the torsion angle of the C–S–O–Cd fragments. In the mononuclear $[Cd(2,2'\text{-bpy})_2(H_2O)(peds)]\cdot 4H_2O$, Cd^{2+} is coordinated by four nitrogen atoms from two 2,2′-bpy ligands in *cis* fashion, one water molecule and one $–SO_3^-$ oxygen atom of the peds anion. The $–SO_3^-$ group on the other end of the peds ligand is not anchored by any covalent bond. The overall structure of $[Cd(2,2'\text{-bpy})_2(H_2O)(peds)]\cdot 4H_2O$ is very "polar", carrying positive and negative charges at the metal center and the dangling ligand, respectively. The non-coordinated $–SO_3^-$ group is stabilized by two water molecules by strong hydrogen bonds, as shown in Fig. 31. The peds ligand is highly twisted, with a dihedral angle of 71.1° formed between the two phenyl rings.

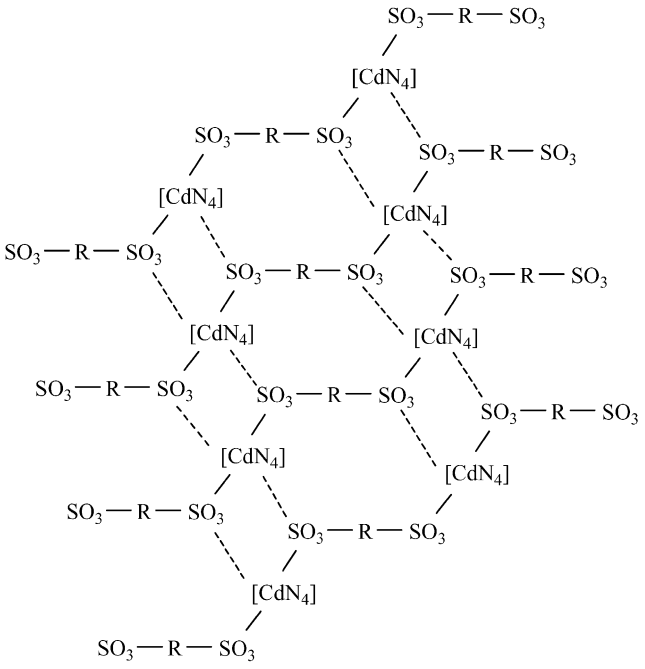

Fig. 30. Schematic plot of the 2D network constructed by hydrogen bonds.

In the dinuclear cluster $[Cd_2(2,2'\text{-bpy})_4(H_2O)_2(1,5nds)](1,5nds)\cdot 4H_2O$, each of the Cd^{2+} ions has a similar coordination environment to that observed in the mononuclear $[Cd(2,2'\text{-bpy})_2(H_2O)(peds)]\cdot 4H_2O$. However, both SO_3^- groups of the 1,5nds ligand coordinate with Cd^{2+} monodentately, in *trans* fashion, resulting in a dinuclear cation, as shown in Fig. 32a. The two 2,2′-bpy and naphthalene planes are almost coplanar. The free 1,5nds anions connect two dinuclear clusters via hydrogen bonds formed by the coordinated water molecules and $–SO_3^-$ oxygen atoms, extending the dinuclear clusters into 1D chains, as shown in Fig. 32b.

In the neutral dinuclear cluster $[Cd(cyclam)(1,5nds)]_2$, Cd^{2+} is 6-coordinated by four nitrogen atoms from one cyclam ligand in *cis* fashion and two SO_3^- oxygen atoms from two different 1,5nds anions. The Cd^{2+} ions are double-bridged by two μ^2–SO_3^- groups, resulting a dinuclear cluster, as illustrated in Fig. 33a. It is interesting to note that when the metal ion in the polymeric $[M(cyclam)(1,5nds)]_n$ ($M = Cu^{2+}$ [100] and Ni^{2+} [104]) was substituted by Cd^{2+}, the resulting structure changes from 1D chain to a dinuclear

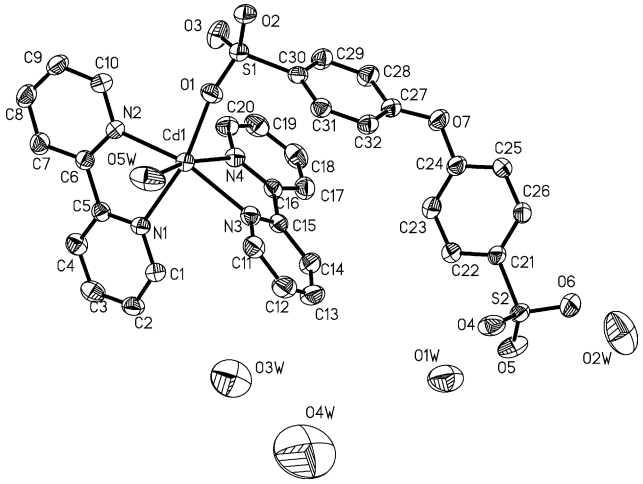

Fig. 31. $[Cd(2,2'\text{-bpy})_2(H_2O)(peds)]\cdot 4H_2O$.

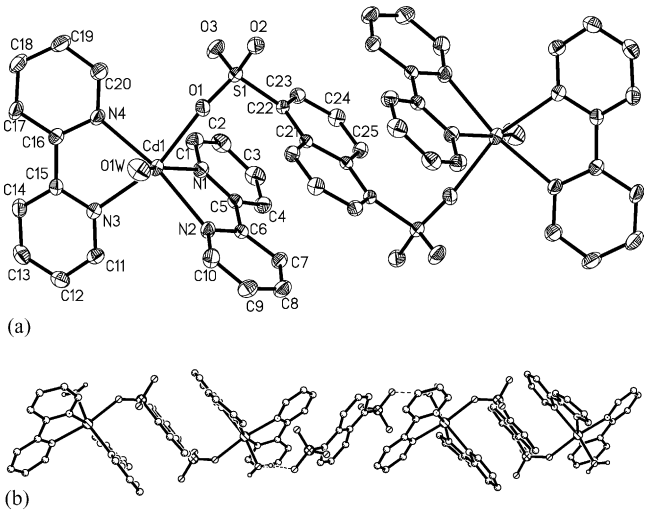

Fig. 32. The coordination structure (a) and packing (b) of $[Cd_2(2,2'\text{-bpy})_4(H_2O)_2(1,5nds)](1,5nds)\cdot 4H_2O$.

cluster. The two non-coordinated $-SO_3^-$ groups of the cluster are anchored by strong intermolecular hydrogen bonds with the amino hydrogen atoms of adjacent clusters, as shown in Fig. 33b, leading to extended 1D chains.

The 1D polymers $\{[Cd(inia)_2(H_2O)_2(2,6nds)]\cdot 4H_2O\}_n$ and $\{[Cd(inia)_2(H_2O)_2(bpds)]\cdot 4H_2O\}_n$ have very similar metal ion coordination structures and packing arrangement, as shown in Figs. 34 and 35. Two aqua molecules, two isonicotinamide and two $-SO_3^-$ groups coordinate in a *trans* fashion. The 2,6nds/bpds anions behave as bifunctional spacers coordinated to two Cd(II) centers, resulting in step-like 1D coordination polymers. Adjacent chains are connected by N–H...O hydrogen bonds formed between amide moieties and sulfonate groups, leading to extended 2D sheets. The extended 2D layer structures in $\{[Cd(inia)_2(H_2O)_2(2,6nds)]\cdot 4H_2O\}_n$ and $\{[Cd(inia)_2(H_2O)_2(bpds)]\cdot 4H_2O\}_n$ are very similar, despite the fact that the length of the spacer are 8.49 and 10.66 Å in 2,6nds and bpds, respectively. In other words, the directing forces for the assembly of the polymers, $\{[Cd(inia)_2(H_2O)_2(2,6nds)]\cdot 4H_2O\}_n$ and $\{[Cd(inia)_2(H_2O)_2(bpds)]\cdot 4H_2O\}_n$, into 2D structures are the same, similar to the supramolecular synthon documented above for the Cd(N4)(nds/bpds) analogs.

In the 1D knotted chain $\{[Cd_2(inia)_4(H_2O)_3(peds)_2]\cdot 2H_2O\}_n$, there are two independent Cd^{2+} ions with different coordination geometry in the asymmetric unit. Cd(1) is coordinated by one water molecule, two nicotinamide nitrogen atoms and three sulfonate oxygen atoms, and Cd(2) by two water molecules, two nicotinamide nitrogen atoms and two sulfonate oxygen atoms, as shown in Fig. 36a. Each of the Cd^{2+} ions are double-bridged by two μ^2–SO_3^- groups, resulting two 8-membered-ring dinuclear clusters. The clusters are linked by peds spacers into 1D knotted chains, as shown in Fig. 36b. Both the spacer and terminal peds anions in the asymmetric unit coordinate with Cd^{2+} in an asymmetric fashion. One served as a spacer displays a μ^2 μ^1 mode, one end μ^2-bridging and the other end monodentate; while the second peds coordinates only with one end as a μ^2-bridge and the other end free.

The solid-state structures of the above complexes show that all the six possible coordination modes of disulfonate

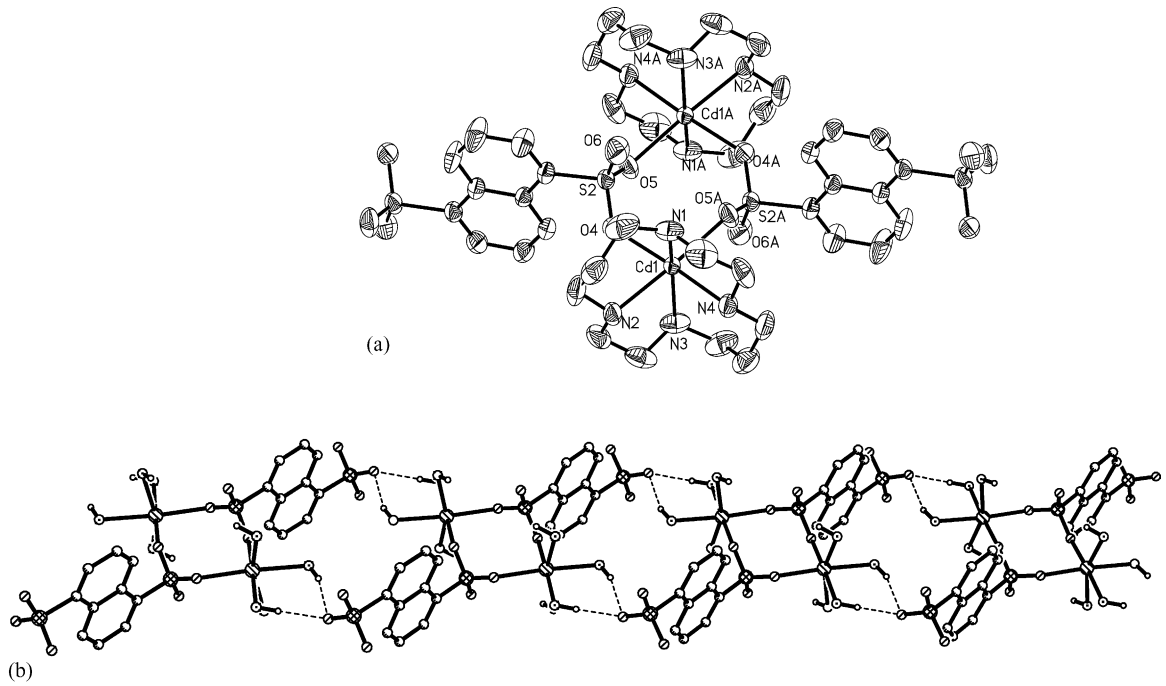

Fig. 33. The coordination structure (a) and extended 1D chain formed by hydrogen bonds in $[Cd(cyclam)(1,5nds)]_2$.

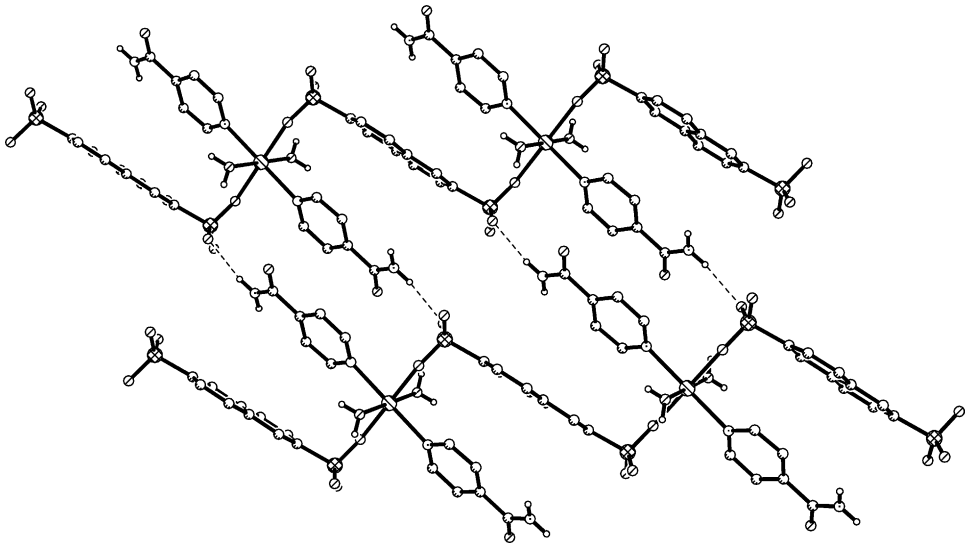

Fig. 34. $\{[Cd(inia)_2(H_2O)_2(2,6nds)]\cdot 4H_2O\}_n$.

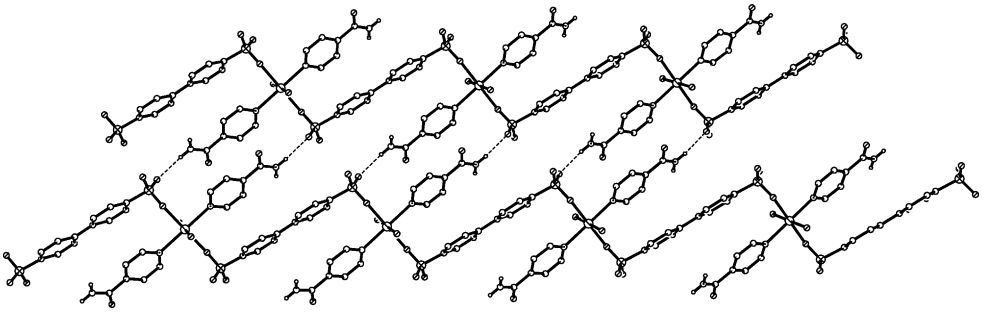

Fig. 35. $\{[Cd(inia)_2(H_2O)_2(bpds)]\cdot 4H_2O\}_n$.

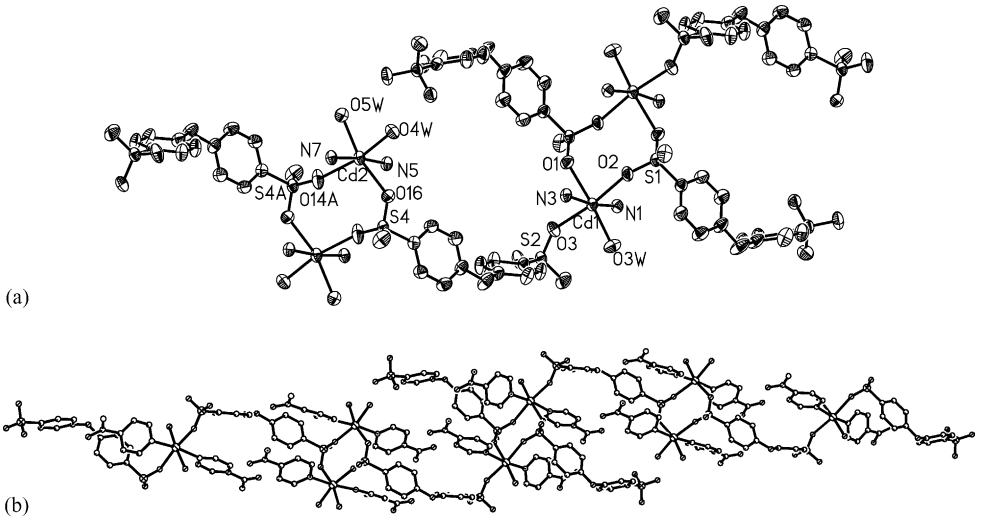

Fig. 36. Coordination (a) and 1D structure (b) of $\{[Cd_2(inia)_4(H_2O)_3(peds)_2]\cdot 2H_2O\}_n$.

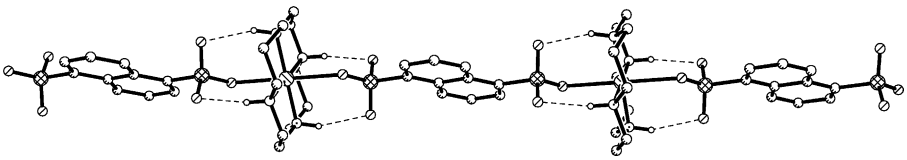

Fig. 37. $\{[Ni(cyclam)(1,5nds)]\cdot(1/3)H_2O\}_n$.

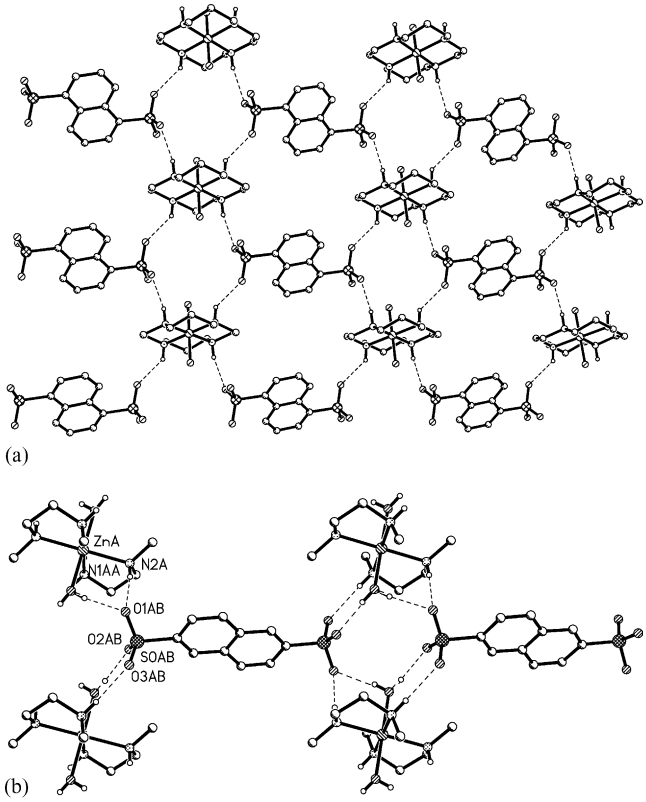

Fig. 38. $[Co(cyclam)(H_2O)_2](1,5nds)\cdot 2H_2O$ (a) and $Zn(N\text{-meen})_2(H_2O)_2](2,6nds)$ (b).

ions shown in Fig. 30 could be adopted with different N-containing auxiliary ligands. Furthermore, the $-SO_3^-$ oxygen atoms are involved in extensive intermolecular hydrogen bonds which could be directive and leading to extended structures with higher order of dimensionalities.

3.4. Other transition metals

In an effort to obtain the structural analogs of Cu^{2+} and Cd^{2+} with metal–sulfonate interactions, the mixed-ligand strategy is applied to Ni^{2+}, Co^{2+} and Zn^{2+} ions. Nevertheless, except in $\{[Ni(cyclam)(1,5nds)]\cdot(1/3)H_2O\}_n$ [104] where a weak Ni-sulfonate contact is observed, all the other compounds are obtained as amine/water coordinated metal cations with the sulfonate as the counter-anions. X-ray structural analyses show that their structures are $[Ni(H_2O)_6](1,5nds)$, $[Ni(en)_2(H_2O)_2](1,5nds)\cdot 2H_2O$, $[Ni(tren)(H_2O)_2](1,5nds)\cdot H_2O$, $[Ni(dien)_2](1,5nds)\cdot 2H_2O$ [103], $[Ni(N\text{-meen})_2(H_2O)_2](1,5nds)$, $[Ni(N,N'\text{-meen})_2(H_2O)_2](1,5nds)\cdot H_2O$, $[Ni(N,N'\text{-meen})_2(H_2O)_2](2,6nds)$, $[Ni(inia)_2(H_2O)_4](1,5nds)\cdot 2H_2O$ [109] for the Ni^{2+} compounds, $[Zn(dien)_2](1,5nds)$, $[Zn(dpn)_3](1,5nds)\cdot H_2O$, $[Zn(N,N'\text{-meen})_2(H_2O)_2](1,5nds)\cdot H_2O$, and $Zn(N\text{-meen})_2(H_2O)_2](2,6nds)$ [109] for the Zn^{2+} compounds, and $[Co(cyclam)(H_2O)_2](1,5nds)\cdot 2H_2O$ [104]. As shown in Fig. 37, $\{[Ni(cyclam)(1,5nds)]\cdot(1/3)H_2O\}_n$ is isostructural to its Cu^{2+} analog, with two sulfonate groups coordinated to Ni^{2+} in the axial positions. The distance between the Ni^{2+} and sulfonate is 2.4573(16) Å. As selectively shown in Fig. 38, in all the other complexes, the metal ions are coordinated by the amine ligands and the water molecules with sulfonates as the counter-anions. Extensive hydrogen bonds are formed between the complexes cations and sulfonate anions.

The results summarize above indicate that the coordination strength of divalent transition metal ions toward the sulfonate group increase in the order of $Co^{2+} \sim Zn^{2+} < Ni^{2+} < Cu^{2+} < Cd^{2+}$.

4. Amine interaction properties of layered Cd^{2+} sulfonates

4.1. $[Cd(1,5\text{-nds})(H_2O)_2]_n$

The structure of $[Cd(1,5\text{-nds})(H_2O)_2]_n$ has been discussed above [105]. TGA analysis shows that it is stable until 250 °C when the two coordinated water molecules are released. Its amine uptake properties were investigated in order to compare the corresponding behavior with that of the well-investigated metal phosphonates [83–89]. The results show that it can selectively absorb ammonia and amines without dehydration and form stable adducts, via solid–vapor reaction at room temperature. As shown in Fig. 39, $[Cd(1,5nds)(H_2O)_2]_n$ can absorb quantitatively ammonia and primary aliphatic amines, but not methanol, ethanol, propanol, acetonitrile and ethyl acetate. Therefore, the uptake of amine is selective.

The C-substitution on the alkyl chain of the amine molecules can alter the absorbing capabilities. For instance, $[Cd(1,5nds)(H_2O)_2]_n$ absorbs 4 equiv. of $C_3H_7NH_2$ and 3 equiv. of iso-$C_3H_7NH_2$. However, it absorbs the same amount of $C_4H_9NH_2$ and iso-$C_4H_9NH_2$ in molar ratio of 1:3. Therefore, β-substitution on the C-atom has no obvious impact, while α-substitution decreases the intercalation capability noticeably.

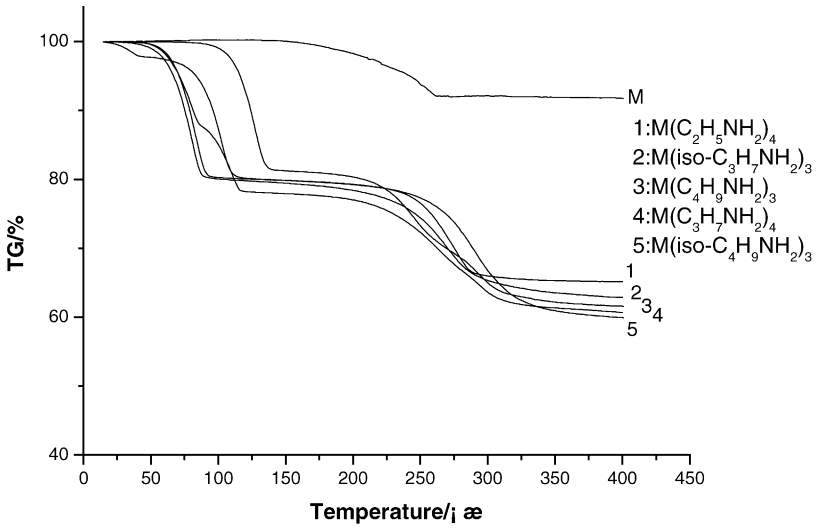

Fig. 39. TGA of the amine adducts of $[Cd(1,5nds)(H_2O)_2]_n$ (M) showing the amines released at two well-defined temperature ranges.

$[Cd(1,5nds)(H_2O)_2]_n$ can also absorb up to 2 molar equivalents of secondary amine $(C_2H_5)_2NH$. However, no absorption is observed for $(C_2H_5)_3N$ and the aromatic amines $PhNH_2$ and $PhCH_2NH_2$. Also, in order to test the interaction preference, the absorption experiment of $[Cd(1,5nds)(H_2O)_2]_n$ with mixed amines of $CH_3NH_2/C_2H_5NH_2$ and $C_2H_5NH_2/(C_2H_5)_2NH$ were also conducted, and only $C_2H_5NH_2$ was detected from the TGA-IR spectra. The XRD spectra of the resulting amine adducts also matched that observed for $M(C_2H_5NH_2)_4$, indicating that $[Cd(1,5nds)(H_2O)_2]_n$ shows preferential absorption behavior.

The amine interaction process of the matrix compound involves both coordinative and non-coordinative interactions. In the $C_2H_5NH_2$ and $C_3H_7NH_2$ adducts, in which maximum amount of amines are found, TGA-IR analyses show that the amines are released in two separated steps, while the water molecules are released at a much lower temperature than the matrix compound $[Cd(1,5nds)(H_2O)_2]_n$. This observation indicates that the intercalation process could be that two amine molecules substitute the two coordinated water molecules, while the other two amine molecules are anchored into the expanded inter-layered spaces, most probably via forming hydrogen bonds with the sulfonate oxygen atoms of the matrix compound. Based upon the 3D TGA-IR spectra, there are amines released at much higher temperature than their corresponding boiling points, suggesting that coordinative intercalations commonly occur in all the cases studied.

All the amine adducts are crystalline materials with different phases and could have better crystallinity than the matrix compound. The PXRD patterns are very similar for amine adducts obtained during different trials, before/after treatment with methanol/ether, indicating that these adducts have well-defined and stable structures which could be quantitatively reproduced. Moreover, as shown in Fig. 40, the adduct process is reversible.

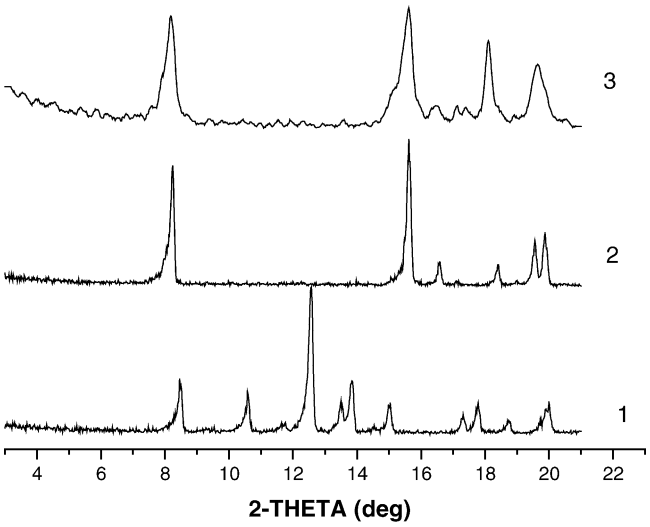

Fig. 40. Feature PXRD patterns at $\theta < 10.5^\circ$ showing the reversible intercalation of $[Cd(1,5nds)_2(H_2O)_2]_n$ with $C_2H_5NH_2$. (1) $C_2H_5NH_2$ adduct of $[Cd(1,5nds)_2(H_2O)_2]_n$; (2) $[Cd(1,5nds)_2(H_2O)_2]_n$; (3) the $C_2H_5NH_2$ adduct was heated to 280 °C for 2 h, exposed in the air overnight.

In most of the divalent metal phosphates reported, the absorption ratio is 1:1, and only in the case of $Cu(O_3PC_6H_5)$ [86], an extra molar amount of amine is intercalated, most likely via coordinated to Cu^{2+} in the axial positions, while intercalation via other nature of interaction has not been reported in the metal phosphonates. It is quite unusual to observe that $[Cd(1,5nds)(H_2O)_2]_n$ can absorb up to 4 molar equivalents of amine and form stable adducts, without dehydration before the solid–vapor reaction.

4.2. $[Cd(\mu_2\text{-}p\text{-}N,O\text{-}NH_2C_6H_4SO_3)_2(H_2O)_2]_n$

$[Cd(\mu_2\text{-}p\text{-}N,O\text{-}NH_2C_6H_4SO_3)_2(H_2O)_2]_n$ is a layered coordination compound with similar 2D structure to that

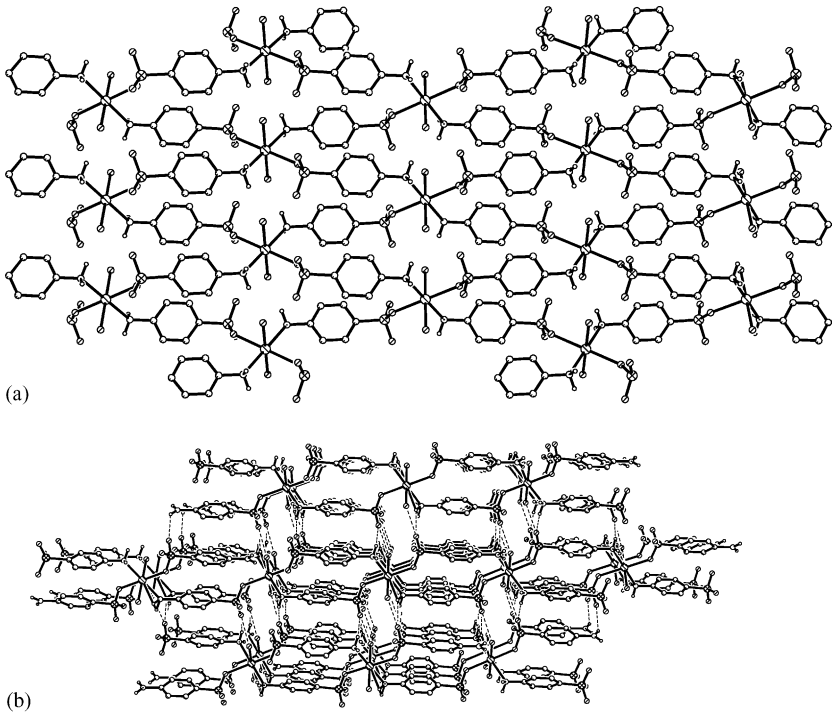

Fig. 41. 2D (a) and packing (b) structures of $[Cd(\mu_2\text{-}p\text{-}N,O\text{-}NH_2C_6H_4SO_3)_2(H_2O)_2]_n$.

adopted by $[Cd(1,5nds)(H_2O)_2]_n$. The solid–vapor reactions between crystalline $[Cd(\mu_2\text{-}p\text{-}N,O\text{-}NH_2C_6H_4SO_3)_2(H_2O)_2]_n$ and a series of volatile amines were investigated and the corresponding amine adducts were characterized by EA, TGA, PXRD and IR [106]. Among them, the $C_2H_5NH_2$ and $C_3H_7NH_2$ adducts, namely $[Cd(C_2H_5NH_2)_4(H_2O)_2](H_2NC_6H_4SO_3)_2$ and $[Cd(C_3H_7NH_2)_4(p\text{-}O\text{-}H_2NC_6H_4SO_3)_2](C_3H_7NH_2)$, grew into single crystals in situ of the solid–vapor reaction processes and their crystal structures were characterized. In both cases, 4 molar amounts of amine molecules coordinate to Cd^{2+} via replacing the $p\text{-}N,O\text{-}NH_2C_6H_4SO_3^-$ ligands or coordinated water molecules. The single-phase product suggests that the solid–vapor reaction between metal sulfonate and volatile alkylamines could be used as a green process to synthesize monoamine-coordinated Cd^{2+} complexes without using any solvent and routine separation.

The crystal structure of $[Cd(\mu_2\text{-}p\text{-}N,O\text{-}NH_2C_6H_4SO_3)_2(H_2O)_2]_n$ is shown in Fig. 41a. Its Co^{2+} and Zn^{2+} analogs have been reported and all three of them have similar coordination and 2D structures [45]. The $p\text{-}NH_2C_6H_4SO_3^-$ anions behave as μ^2 bridging ligands to produce a 2D layered structure. Inter-layered hydrogen bonds formed between the coordinated water molecules and the $–NH_2$ groups with the free $–SO_3^-$ oxygen atoms generate an extended 3D structure, as shown in Fig. 41b, which is very similar to that of $[Cd(1,5nds)(H_2O)_2]_n$ [102]. $[Cd(\mu_2\text{-}p\text{-}N,O\text{-}NH_2C_6H_4SO_3)_2(H_2O)_2]_n$ is stable until 100 °C when the water molecules are released. The dehydrated compound $[Cd(\mu_2\text{-}p\text{-}N,O\text{-}NH_2C_6H_4SO_3)_2]_n$ is also a crystalline material, with the inter-layer distance decreased from 9.37 Å in $[Cd(\mu_2\text{-}p\text{-}N,O\text{-}NH_2C_6H_4SO_3)_2(H_2O)_2]_n$ to 8.77 Å in $[Cd(\mu_2\text{-}p\text{-}N,O\text{-}NH_2C_6H_4SO_3)_2]_n$. The dehydration process of $[Cd(\mu_2\text{-}p\text{-}N,O\text{-}NH_2C_6H_4SO_3)_2(H_2O)_2]_n$ is reversible.

$[Cd(\mu_2\text{-}p\text{-}N,O\text{-}NH_2C_6H_4SO_3)_2(H_2O)_2]_n$ does not react with NH_3, $(C_2H_5)_2NH$, $PhNH_2$, pyridine, as well as CH_3OH, $CH_3COOC_2H_5$ and HCl, indicating that the reaction of $[Cd(\mu_2\text{-}p\text{-}N,O\text{-}NH_2C_6H_4SO_3)_2(H_2O)_2]_n$ with primary amines is selective. $[Cd(\mu_2\text{-}p\text{-}N,O\text{-}NH_2C_6H_4SO_3)_2(H_2O)_2]_n$ can quantitatively absorb primary alkylamines. Especially, $[Cd(\mu_2\text{-}p\text{-}N,O\text{-}NH_2C_6H_4SO_3)_2(H_2O)_2]_n$ can take up to 4 equiv. of CH_3NH_2 and $C_2H_5NH_2$, 5 equiv. of $C_3H_7NH_2$. It is noted that there is a sharp decrease in the molar amount of amines adducted to $[Cd(\mu_2\text{-}p\text{-}N,O\text{-}NH_2C_6H_4SO_3)_2(H_2O)_2]_n$ from 5 mol for $C_3H_7NH_2$ to 0.5 mol for iso-$C_3H_7NH_2$, and 0.5–1.5 mol for the $C_4H_9NH_2$ isomers. All the ammine adducts are crystalline materials. TGA results, shown in Fig. 42, reveal that the CH_3NH_2, $C_2H_5NH_2$ and $C_3H_7NH_2$ adducts release amine molecules in single steps, well before the decomposition of the framework around 350 °C.

Both $C_2H_5NH_2$ and $C_3H_7NH_2$ adducts grow into single crystals in situ in solid–vapor reactions. X-ray structural analysis shows that 4 equiv. of $C_2H_5NH_2$ substitute the $p\text{-}NH_2C_6H_4SO_3^-$ ligands from the Cd^{2+} coordination sphere, while the water molecules remain coordinated to the metal center, resulting in $[Cd(C_2H_5NH_2)_4(H_2O)_2](p\text{-}NH_2C_6H_4SO_3)$, as shown in Fig. 43. The crystal structure of the $C_3H_7NH_2$ adduct, $[Cd(C_3H_7NH_2)_4(p\text{-}O\text{-}H_2NC_6H_4SO_3)_2](C_3H_7NH_2)$ is shown in Fig. 44a. Four

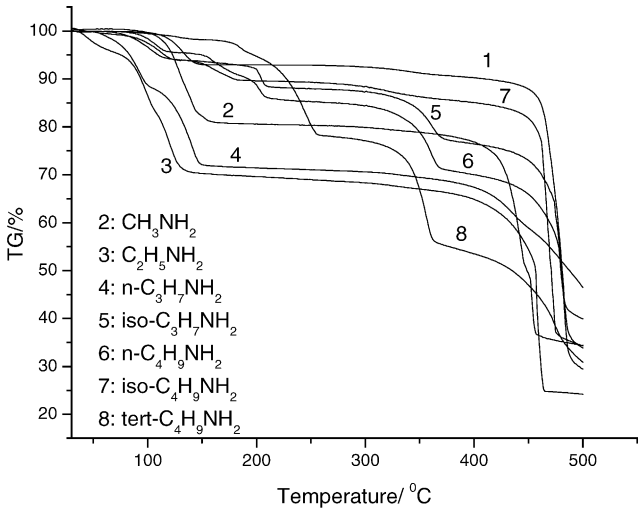

Fig. 42. TGA of the amine adducts of $[Cd(\mu_2\text{-}p\text{-}N,O\text{-}NH_2C_6H_4SO_3)_2(H_2O)_2]_n$.

equivalents of amine replace the two coordinated water molecules and $-NH_2$ groups of the two $p\text{-}NH_2C_6H_4SO_3^-$ ligands. The sulfonate group remains coordinated to Cd^{2+}, with the Cd–O distance expanded significantly from 2.294(2) Å in $[Cd(\mu_2\text{-}p\text{-}N,O\text{-}NH_2C_6H_4SO_3)_2(H_2O)_2]_n$ to 2.474(4) and 2.453(4) Å in $[Cd(C_3H_7NH_2)_4(p\text{-}O\text{-}H_2NC_6H_4SO_3)_2]C_3H_7NH_2$). Interestingly, molecules pack along the crystallographic *a*-axis and form void space of 200 $Å^3$ per unit cell, which accommodates one free amine molecule, as shown in Fig. 44b. In other words, $[Cd(\mu_2\text{-}p\text{-}N,O\text{-}NH_2C_6H_4SO_3)_2(H_2O)_2]_n$ can take up to 5 equiv. of $C_3H_7NH_2$ and form crystalline $[Cd(C_3H_7NH_2)_4(p\text{-}O\text{-}H_2NC_6H_4SO_3)_2](C_3H_7NH_2)$. Both substitution and inclusion reactions occur during the reaction process.

The absorption of guest molecules by a crystalline material always causes considerable stress and intermolecular reorganization in the metal-organic framework and the loss of the crystallinity. As a consequence, the characterization of the solid-state structures becomes quite challenging. One common approach to overcome this problem is to grow single crystals of the targeted compound from solvent and compare the simulated PXRD pattern with that of the reaction product. This method is only achievable when the targeted compound can be crystallized and the phases obtained from solid-state reaction and from solution are the same. Therefore, the growth of single crystals in situ of a solid–vapor reaction process observed in $[Cd(\mu_2\text{-}p\text{-}N,O\text{-}NH_2C_6H_4SO_3)_2(H_2O)_2]_n$, which makes direct structural characterization possible, is unique.

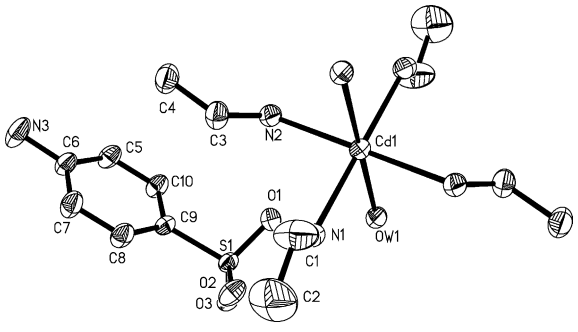

Fig. 43. $[Cd(C_2H_5NH_2)_4(H_2O)_2](H_2NC_6H_4SO_3)_2$.

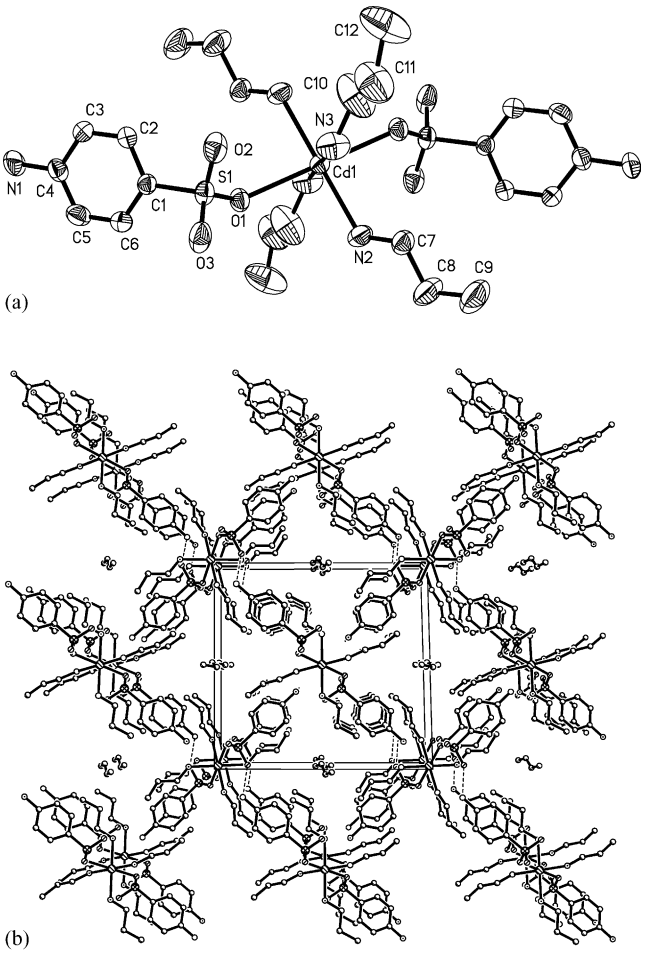

Fig. 44. Coordination structure (a) and packing (b) of $[Cd(C_3H_7NH_2)_4(p\text{-}O\text{-}H_2NC_6H_4SO_3)_2](C_3H_7NH_2)$.

As shown in Fig. 45, the solid–vapor reaction between $[Cd(\mu_2\text{-}p\text{-}N,O\text{-}NH_2C_6H_4SO_3)_2(H_2O)_2]_n$ and $C_2H_5NH_2$, namely the substitution reaction including the breakdown and formation of four coordinative bonds, is completely reversible at room conditions. Similar amine-releasing processes at room temperature are observed in all the other amine adducts. In the cases of both the CH_3NH_2 and $C_3H_7NH_2$ adducts, the phases obtained after loss of all the amine molecules have to be exposed to water moisture in order to gain the phase identical to that of $[Cd(\mu_2\text{-}p\text{-}N,O\text{-}NH_2C_6H_4SO_3)_2(H_2O)_2]_n$. The amine-releasing process could also be accelerated by heating to 150–200 °C.

Complex $[Cd(\mu_2\text{-}p\text{-}N,O\text{-}NH_2C_6H_4SO_3)_2(H_2O)_2]_n$ shows distinct reactivity towards $C_2H_5NH_2$ and $C_3H_7NH_2$. Four equivalents of $C_2H_5NH_2$ exclude the $p\text{-}NH_2C_6H_4SO_3^-$ ligands from the Cd^{2+} coordination sphere. But this does not occur in the case of $C_3H_7NH_2$ reaction, where the sulfonate

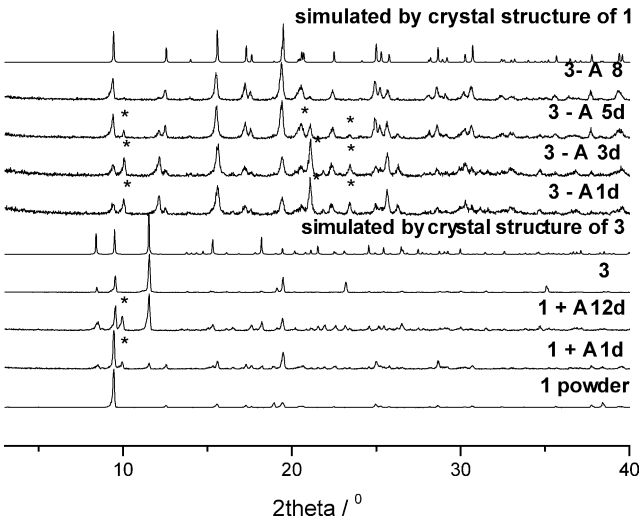

Fig. 45. PXRD tracking the reversible transformations between [Cd(μ_2-*p*-*N*,*O*-$NH_2C_6H_4SO_3$)$_2$(H_2O)$_2$]$_n$ (1) and the $C_2H_5NH_2$ adduct **3**. A = $C_2H_5NH_2$ vapor. Reflections contributed by the third phase are marked by *.

groups of the *p*-$NH_2C_6H_4SO_3^-$ ligands still remain coordinated to Cd^{2+}. Further experiments are required in order to decipher this behavior, which could be caused by steric and electronic factors. On the other hand, based upon what we have documented about the readily modified sulfonate coordination mode due to its weak coordination nature, what is being observed here is not unexpected.

The readily achieved transformations between [Cd(μ_2-*p*-*N*,*O*-$NH_2C_6H_4SO_3$)$_2$·(H_2O)$_2$]$_n$ and its amine adducts could be explained by the compatible coordination strength of the –NH_2 and –SO_3^- groups of the $NH_2C_6H_4SO_3^-$ ligand, the –NH_2 group of the alkylamine and the water molecule. By nature, the reaction process of metal sulfonate with amine vapor could be understood as a solid-state substitution reaction driven by Lewis acid–base interactions. Experimental results show that cadmium(II) salts other than the sulfonates, such as $CdCl_2$ and $CdCO_3$, do not react with amine vapor under the same reaction condition investigated for [Cd(μ_2-*p*-*N*,*O*-$NH_2C_6H_4SO_3$)$_2$(H_2O)$_2$]$_n$ and [Cd(1,5nds)(H_2O)$_2$]$_n$, revealing that the sulfonate group is critical to drive the amine intercalating process.

5. Summary and conclusions

We have demonstrated that by employing aromatic disulfonate anions as ligands, sulfonate-coordinated main group and transition metal complexes can be obtained from aqueous solution. The cooperative multiple metal–sulfonate interactions direct the construction of the stable frameworks with various dimensionalities. Diverse coordination modes of sulfonates are observed, indicative of the flexible coordination feature of the sulfonate group. Moreover, the order of the coordination strength of the alkali and alkaline earth metals towards sulfonates, namely $Li^+ < Na^+ < K^+$ and $Mg^{2+} < Ca^{2+} < Sr^{2+} \sim Ba^{2+}$, is illustrated satisfactorily by the solid-state structures of the 1,5-naphthalenedisulfonate salts. The order of the coordination strength of transition metal ions is illustrated by comparing the solid-state structures of metal sulfonates with similar component but different sulfonate coordination behavior. Especially, the different coordination modes observed in the series complexes M(cyclam)(1,5nds)·*n*H_2O (M = Co^{2+}/μ^0, Ni^{2+}/μ^1, Cu^{2+}/μ^1 and Cd^{2+}/μ^2) serve as a unique example to demonstrate the coordination strength increase in the order $Co^{2+} < Ni^{2+} < Cu^{2+} < Cd^{2+}$.

Layered metal sulfonates can display interesting functional properties, such as the reversible and selective uptake of amine at room temperature without dehydration. Such kind of reversible vapor or gas uptake property has attracted more and more attention recently due to potential application as chemical sensors for toxic gases or volatile organic compounds [110]. Moreover, the easy replacement of the sulfonate group can be utilized to synthesize novel compounds, such as monoamine-coordinated metal complexes, which are otherwise difficult to obtain from solvent reaction, via solid–vapor reactions between metal sulfonates and volatile ligands.

The negatively charged –SO_3^- oxygen atoms can also form strong and directed hydrogen bonds, constructing well-organized extended coordination frameworks with functional properties. The N–H···O types of hydrogen bonds formed by guanidinium and sulfonates have been investigated heavily in organic crystal engineering [111]. While recently, Shimizu's group has reported a series of inclusion solids constructed by the second-sphere interaction of the sulfonate anions and the ammonium-coordinated metal cations [112]. With the infinite number of organic ligands available and the rich and tunable coordination chemistry displayed by sulfonates, we believe that further studies on the solid-state chemistry of metal sulfonates will be rewarded by structures with interesting frameworks, and, most importantly, a comprehensive understanding of the coordination behavior of sulfonates, which is crucial for designing functional metal sulfonate materials.

Acknowledgement

We thank the financial support from the National Natural Science Foundation of China (Grant Nos. 20271053 and 20131020).

References

[1] A.P. Côté, G.K.H. Shimizu, Coord. Chem. Rev. 245 (2003) 49.
[2] G.A. Lawrence, Chem. Rev. 86 (1986) 17.
[3] J.L. Atwood, L.J. Barbour, M.J. Hardie, C.L. Raston, Coord. Chem. Rev. 222 (2001) 3.
[4] A. Clearfield, Prog. Inorg. Chem. 47 (1998) 371.

[5] J. Cai, C.H. Chen, C.Z. Liao, X.L. Feng, C.M. Chen, Acta Crystallogr. Sect. B 57 (2001) 520.
[6] J. Cai, C.-Z. Liao, unpublished results.
[7] G.K.H. Shimizu, G.D. Enright, C.I. Ratcliffe, G.S. Rego, J.L. Reid, J.A. Ripmeester, Chem. Mater. 10 (1998) 3282.
[8] G.K.H. Shimizu, G.D. Enright, C.I. Ratcliffe, K.F. Preston, J.L. Reid, J.A. Ripmeester, Chem. Commun. (1999) 1485.
[9] R. Ruther, F. Huber, H. Preut, J. Organomet. Chem. 295 (1985) 21.
[10] H. Preut, R. Ruther, F. Huber, Acta Crystallogr. C 42 (1986) 1154.
[11] R. Ruther, F. Huber, H. Preut, Z. Anorg, Allg. Chem. 539 (1986) 110.
[12] R. Ruther, F. Huber, H. Preut, Angew. Chem. Int. Ed. 26 (1987) 906.
[13] V.V. Sharutin, O.K. Sharutina, L.P. Panova, V.K. Bel'sky, Zh. Obshch. Khim. (Russ.) (Russ. J. Gen. Chem.) 67 (1997) 1531.
[14] V. Sharutin, O.K. Sharutina, N.V. Nasonova, I.A. Ivashchik, D.B. Krivolapov, A.T. Gubaidullin, I.A. Litvinov, Izv. Akad. Nauk SSSR Ser. Khim. (Russ.) (Russ. Chem. Bull.) (1999) 2346.
[15] V.V. Sharutin, O.K. Sharutina, T.A. Tarasova, A.N. Kharsika, V.K. Bel'sky, Zh. Obshch. Khim. (Russ.) (Russ. J. Gen. Chem.) 69 (1999) 1979.
[16] V.V. Sharutin, O.K. Sharutina, T.A. Tarasova, T.A. Kovaleva, V.K. Bel'sky, Zh. Obshch. Khim. (Russ.) (Russ. J. Gen. Chem.) 70 (2000) 1311.
[17] V.V. Sharutin, O.K. Sharutina, T.P. Platonova, A.P. Pakusina, D.B. Krivolapov, A.T. Gubaidullin, I.A. Litvinov, Zh. Obshch. Khim. (Russ.) (Russ. J. Gen. Chem.) 70 (2000) 1668.
[18] V.V. Sharutin, A.P. Pakusina, V.S. Senchurin, A.V. Gerasimenko, E.A. Gerasimenko, Koord. Khim. (Russ.) (Coord. Chem.) 28 (2002) 577.
[19] V.V. Sharutin, O.K. Sharutina, I.V. Egorova, V.S. Senchurin, A.N. Zakharova, V.K. Bel'sky, Zh. Obshch. Khim. (Russ.) (Russ. J. Gen. Chem.) 69 (1999) 1470.
[20] S.W. Ng, V.G.K. Das, J. Crystallogr. Spectrosc. Res. 22 (1992) 507.
[21] A. Ruzicka, A. Lycka, R. Jambor, P. Novak, I. Cisarova, M. Holcapek, M. Erben, J. Holecek, Appl. Organomet. Chem. 17 (2003) 168.
[22] R. Schibli, R. Alberto, U. Abram, S. Abram, A. Egli, P.A. Schubiger, T.A. Kaden, Inorg. Chem. 37 (1998) 3509.
[23] G. Fachinetti, T. Funaioli, F. Marchetti, J. Organomet. Chem. 498 (1995) C20.
[24] U. Kolle, R. Gorissen, T. Wagner, Chem. Ber. 128 (1995) 911.
[25] A. Vigalok, D. Milstein, Organometallics 19 (2000) 2341.
[26] A.A.D. Tulloch, S. Winston, A.A. Danopoulos, G. Eastham, M.B. Hursthouse, J. Chem. Soc., Dalton Trans. (2003) 699.
[27] D. Rais, D.M.P. Mingos, R. Vilar, A.J.P. White, D.J. Williams, J. Organomet. Chem. 652 (2002) 87.
[28] I.L. Eremenko, V.I. Bakhmutov, F. Ott, H. Berke, Zh. Neorg. Khim. (Russ.) (Russ. J. Inorg. Chem.) 38 (1993) 1653.
[29] Y. Bankovsky, J. Lejejs, E. Silina, V. Belsky, V. Zavodnik, L. Pech, Latv. Khim. Z. (Latvian J. Chem.) (1992) 461.
[30] S. Petit, S. Ammor, G. Coquerel, C. Mayer, G. Perez, J.-M. Dance, Eur. J. Solid State Inorg. Chem. 30 (1993) 497.
[31] C. Aller, J. Castro, P. Perez-Lourido, E. Labisbal, J.A. Garcia-Vazquez, Acta Crystallogr. C 58 (2002) 155.
[32] S. Francis, P.T. Muthiah, G. Bocelli, A. Cantoni, Acta Crystallogr. E 59 (2003) 87.
[33] S.B. Raj, P.T. Muthiah, U. Rychlewska, B. Warzajtis, G. Bocelli, R. O'lla, Acta Crystallogr. E 59 (2003) 46.
[34] G. Smith, B.A. Cloutt, D.E. Lynch, K.A. Byriel, C.H.L. Kennard, Inorg. Chem. 37 (1998) 3236.
[35] G.K.H. Shimizu, G.D. Enright, C.I. Ratcliffe, J.A. Ripmeester, Chem. Commun. (1999) 461.
[36] L. Carlucci, G. Ciani, D.M. Proserpio, S. Rizzato, J. Solid State Chem. 152 (2000) 211.
[37] M. Baumeister, R. Alberto, K. Ortner, B. Spingler, P.A. Schubiger, T.A. Kaden, J. Chem. Soc., Dalton Trans. 22 (2002) 4143.
[38] P. Rombke, A. Schier, H. Schmidbaur, J. Chem. Soc., Dalton Trans. (2001) 2482.
[39] J.S. Haynes, S.J. Rettig, J.R. Sams, R.C. Thompson, J. Trotter, Can. J. Chem. 64 (1986) 429.
[40] M.R. Barton, Y. Zhang, J.D. Atwood, J. Coord. Chem. 55 (2002) 969.
[41] B.J. Coe, C.I. McDonald, R.L. Beddoes, Polyhedron 17 (1998) 1997.
[42] F. Benetollo, R. Bertani, G. Bombieri, L. Toniolo, Inorg. Chim. Acta 233 (1995) 5.
[43] C.S. Weinert, N. Prokopuk, S.M. Arendt, C.L. Stern, D.F. Shriver, Inorg. Chem. 40 (2001) 5162.
[44] B.J. Gunderman, P.J. Squattrito, S.N. Dubey, Acta Crystallogr. C 52 (1996) 1131.
[45] V. Shakeri, S. Haussuhl, Z. Kristallogr. 198 (1992) 165.
[46] V.C. Gibson, C. Redshaw, W. Clegg, M.R.J. Elsegood, J. Chem. Soc., Dalton Trans. (1997) 3207.
[47] J. Schreuer, Z. Kristallogr. -New Cryst. Struct. 214 (1999) 311.
[48] P. Starynowicz, Acta Crystallogr. C 48 (1992) 1414.
[49] Y. Ohki, Y. Suzuki, M. Nakamura, M. Shimoi, A. Ouchi, Bull. Chem. Soc. Jpn. 58 (1985) 2968.
[50] Y. Ohki, Y. Suzuki, T. Takeuchi, A. Ouchi, Bull. Chem. Soc. Jpn. 61 (1988) 393.
[51] J. Wu, B. Wang, P. Zheng, G. Xie, Z. Zhang, Y. Gu, Chin. J. Inorg. Chem. 4 (1988) 116.
[52] D.L. Faithfull, J.M. Harrowfield, M.I. Ogden, B.W. Skelton, K. Third, A.H. White, Aust. J. Chem. 45 (1992) 583.
[53] N.W. Alcock, T.J. Kemp, J. Leciejewicz, Inorg. Chim. Acta 203 (1993) 81.
[54] C. Jones, P.C. Junk, M.K. Smith, R.C. Thomas, Z. Anorg. Allg. Chem. 626 (2000) 2491.
[55] Z. Wang, M. Strobele, K.-L. Zhang, H.-J. Meyer, X.-Z. You, Z. Yu, Inorg. Chem. Commun. 5 (2002) 230.
[56] S.J. Dalgarno, C.L. Raston, J. Chem. Soc., Dalton Trans. (2003) 287.
[57] V. Sharutin, O.K. Sharutina, M.V. Zhitkevich, A.N. Kharsika, T.N. Bliznyuk, A.P. Pakusina, V.K. Bel'sky, Zh. Obshch. Khim. (Russ.) (Russ. J. Gen. Chem.) 70 (2000) 923.
[58] N.S. Husgen, G.A. Luinstra, F. Schaper, K. Schmidt, Inorg. Chem. 37 (1998) 3471.
[59] R. Kapoor, A. Gupta, P. Kapoor, P. Venugopalan, J. Organomet. Chem. 619 (2001) 157.
[60] G. Bernardinelli, E.A.C. Lucken, M. Costines, Z. Kristallogr. 195 (1991) 143.
[61] V.V. Sharutin, O.K. Sharutina, I.I. Pavlushkina, I.V. Egorova, A.P. Pakusina, D.V. Krivolapov, A.T. Gubaidullin, I.A. Litvinov, Zh. Obshch. Khim. (Russ.) (Russ. J. Gen. Chem.) 71 (2001) 87.
[62] F. Huber, J. Remer, M. Schurmann, Acta Crystallogr. C 50 (1994) 1913.
[63] G. Smith, J.H. Thomasson, J.M. White, Aust. J. Chem. 52 (1999) 317.
[64] Z.-X. Xie, W. Liu, H.-F. Liu, L.-S. Zheng, Jiegou Huaxue (Chin.) (Chin. J Struct. Chem.) 11 (1992) 139.
[65] G. Smith, D.E. Lynch, C.H.L. Kennard, Inorg. Chem. 35 (1996) 2711.
[66] G.B. Deacon, A. Gitlits, G. Zelesny, D. Stellfeldt, G. Meyer, Z. Anorg. Allg. Chem. 625 (1999) 764.
[67] N. Snejko, C. Cascales, B. Gomez-Lor, E. Gutierrez-Puebla, M. Iglesias, C. Ruiz-Valero, M.A. Monge, Chem. Commun. (2002) 1366.
[68] M.R. Sundberg, R. Sillanpää, Acta Chem. Scand. 47 (1993) 1173.
[69] A. Dyer, An Introduction to Zeolite Molecular Sieves, John Wiley & Sons, New York, 1988.
[70] E.J. Cussen, J.B. Claridge, M.J. Rosseinsky, C.J. Kepert, J. Am. Chem. Soc. 124 (2002) 9574.

[71] H. Li, M. Eddaoudi, M. O'Keeffe, O.M. Yaghi, Nature 402 (1999) 276.
[72] M. Kondo, T. Okubo, A. Asami, S. Noro, T. Yoshitomi, S. Kitagawa, T. Ishii, H. Matsuzaka, K. Seki, Angew. Chem. Int. Ed. 38 (1999) 140.
[73] M.J. Zaworotko, Nature 402 (1999) 242.
[74] O.M. Yaghi, H.-L. Li, D. Davis, D. Richardson, T.L. Groy, Acc. Chem. Res. 31 (1998) 474.
[75] A. Clearfield, Z. Wang, J. Chem. Soc., Dalton Trans. (2002) 2973.
[76] S.S.-Y. Chui, S.M.-F. Lo, J.P.H. Charmant, A.G. Orpen, I.D. Williams, Science 283 (1999) 1148.
[77] L. Pan, K.M. Adams, H.E. Hernandez, X. Wang, C. Zheng, Y. Hattori, K. Kaneko, J. Am. Chem. Soc. 125 (2003) 3062.
[78] X.-M. Zhang, M.-L. Tong, M.-L. Gong, X.-M. Chen, Eur. J. Inorg. Chem. (2003) 138.
[79] L. Pan, H.-M. Liu, S.P. Kelly, X.-Y. Huang, D.H. Olson, J. Li, Chem. Commun. (2003) 854.
[80] L. Pan, H.-M. Liu, X. Lei, X.-Y. Huang, D.H. Olson, N.J. Turro, L. Li, Angew. Chem. Intl. Ed. 42 (2003) 542.
[81] G.S. Papaefstathiou, L.R. MacGillivray, Angew. Chem. Int. Ed. 41 (2002) 2070.
[82] M. Eddoudi, D.B. Moler, H. Li, B. Chen, T.M. Reineke, M. O'Keeffe, O.M. Yaghi, Acc. Chem. Res. 34 (2001) 319.
[83] D.M. Poojary, A. Clearfield, J. Am. Chem. Soc. 117 (1995) 11278.
[84] Y. Zhang, A. Clearfield, Inorg. Chem. 31 (1992) 2821.
[85] G. Cao, V.M. Lynch, L.N. Yacullo, Chem. Mater. 5 (1993) 1000.
[86] Y. Zhang, K.J. Scott, A. Clearfield, Chem. Mater. 5 (1993) 495.
[87] G. Cao, T.E. Mallouk, Inorg. Chem. 30 (1991) 1434.
[88] K.J. Frink, R.-C. Wang, J.L. Colon, A. Clearfield, Inorg. Chem. 30 (1991) 1438.
[89] F. Fredoueil, D. Massiot, P. Janvier, F. Gingl, M. Bujoli-Doeuff, M. Evain, A. Clearfield, B. Bujoli, Inorg. Chem. 38 (1999) 1831.
[90] S.K. Mäkinen, N.J. Melcer, M. Parvez, G.K.H. Shimizu, Chem. Eur. J. 4 (2001) 5176.
[91] A.P. Côté, M.J. Ferguson, K.A. Khan, G.D. Enright, A.D. Kulynych, S.A. Dalrymple, G.K.H. Shimizu, Inorg. Chem. 41 (2002) 287.
[92] A.P. Côté, G.K.H. Shimizu, Chem. Commun. (2001) 251.
[93] J.O. Yu, A.P. Côté, G.D. Enright, G.K.H. Shimizu, Inorg. Chem. 40 (2001) 582.
[94] S.K. Mäkinen, N.J. Melcer, M. Parvez, G.K.H. Shimizu, Chem. Eur. J. 4 (2001) 5176.
[95] B.J. Gundermn, P.J. Squattrito, Inorg. Chem. 33 (1994) 2924.
[96] B.J. Gundermn, P.J. Squattrito, Inorg. Chem. 34 (1995) 2399.
[97] E.J. Kosnic, E.L. McClymont, R.A. Hodder, P.J. Squattrito, Inorg. Chim. Acta 201 (1992) 143.
[98] A.J. Shubnell, E.J. Kosnic, P.J. Squattrito, Inorg. Chim. Acta 216 (1994) 101.
[99] B.J. Gunderman, I.D. Kabell, P.J. Squattrito, S.N. Dubey, Inorg. Chim. Acta 258 (1997) 237.
[100] J. Cai, C.-H. Chen, C.-Z. Liao, J.-H. Yao, X.-P. Hu, X.-M. Chen, J. Chem. Soc., Dalton Trans. (2001) 1137.
[101] J. Cai, C.-H. Chen, X.-L. Feng, C.-Z. Liao, X.-M. Chen, J. Chem. Soc., Dalton Trans. (2001) 2370.
[102] C.-H. Chen, J. Cai, C.-Z. Liao, X.-L. Feng, X.-M. Chen, S.-W. Ng, Inorg. Chem. 41 (2002) 4967.
[103] C.H. Chen, J.W. Cai, X.L. Feng, X.M. Chen, J. Chem. Crystallogr. 31 (2001) 271.
[104] J.W. Cai, C.H. Chen, J.S. Zhou, Chinese J. Inorg. Chem. 19 (2003) 81.
[105] J. Cai, J.-S. Zhou, M.-L. Lin, J. Mater. Chem. 13 (2003) 1806.
[106] J.-S. Zhou, J. Cai, L. Wang, J. Chem. Soc., Dalton Trans. (2004) 1493.
[107] D.M. Poojary, B. Zhang, P. Bellinghausen, A. Clearfield, Inorg. Chem. 35 (1996) 4942.
[108] L. Wang, J. Cai, unpublished results.
[109] C.-H. Chen, J. Cai, unpublished results.
[110] L.H. Poppel, S.G. Bott, A.R. Barron, J. Am. Chem. Soc. 125 (2003) 11006.
[111] K.T. Holman, A.M. Pivovar, A.S. Jennifer, M.D. Ward, Acc. Chem. Res. 34 (2001) 107.
[112] D.S. Reddy, S. Duncan, G.K.H. Shimizu, Angew. Chem. Int. Ed. 42 (2003) 1360.